

OMI PI talk

Pieter Levelt, and OMI
Science Team

27 August 2019, Aura meeting,
Pasadena, USA



OMI
Air Pollution

Non-oxidic NO₂ is an important component of air pollution, and is produced by anthropogenic activities, like fossil fuel burning, and by natural processes, like lightning. This map shows the global distribution of tropospheric NO₂ (NO_x) in the lower part of the atmosphere as observed from 2004 to 2014 by the ozone monitoring instrument (OMI) on the Earth-orbiting satellite. OMI is the only satellite that can distinguish between heavy industry, fossil fuel power plants, biomass burning, oil refineries, and shipping lanes. OMI was built by the Netherlands and related entities as part of NASA's Aura satellite.

Low NO_x High NO_x

William T. Pecora Award 2018
OMI international science team



Royal Netherlands Meteorological Institute
Institute for Environmental Studies

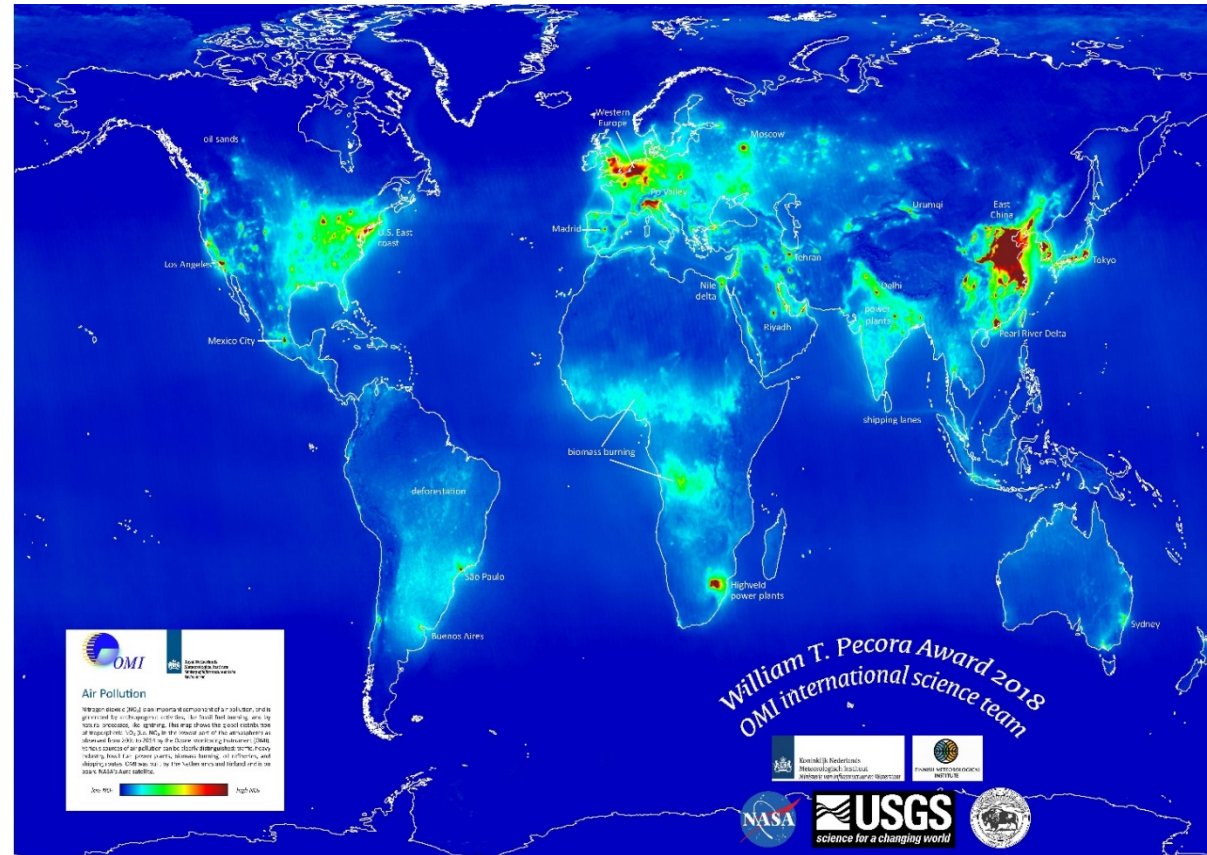


NASA USGS science for a changing world

OMI team receives USGS/NASA 2018 Pecora award

- **OMI team** (Dutch, Finnish, and American scientists) won for “15+ years of sustained team innovation and international collaboration to produce daily global satellite data that revolutionized urban air quality and health research.”
- The **William T. Pecora Award** is presented annually by USGS & NASA to those using remote sensing for making outstanding contributions toward understanding the Earth, educating scientists, informing decision makers or supporting natural or human-induced disaster response.

OMI 2005-2014 tropospheric column NO₂ shows pollution emitted from fossil fuel combustion





OMI Instrument

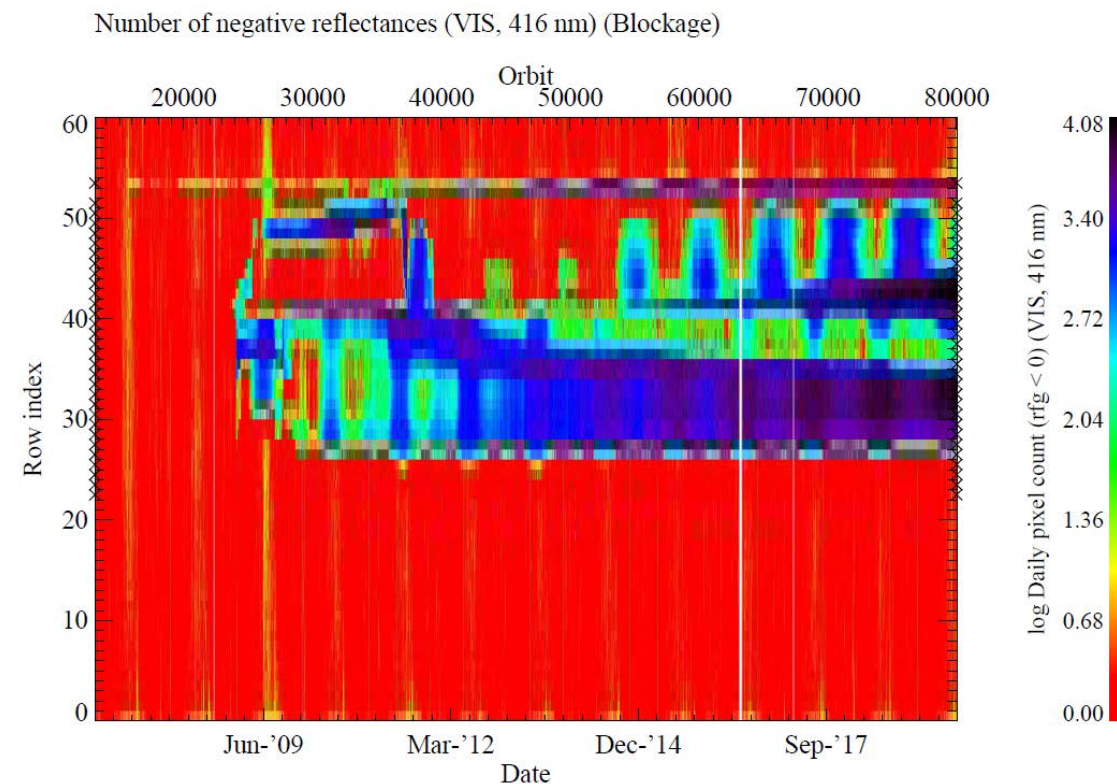
❖ Instrument and Spacecraft

○ Instrument

- Row anomaly since May 2008: status ongoing but appropriate L1B flagging scheme (identifying affected ground pixels) has been implemented
- IAM multi-bit errors on January 2, April 30 and July 30, 2018: No transition to survival mode (yet)
- White Light Source is unstable. Measures were taken that it will not affect OMI operations. Effect on OMI calibration is negligible.

○ Spacecraft

- Formatter/Multiplexer Unit anomaly since Dec. 2007: status ongoing but work-around has been implemented. No impact on the OMI science data.



Calibration Status

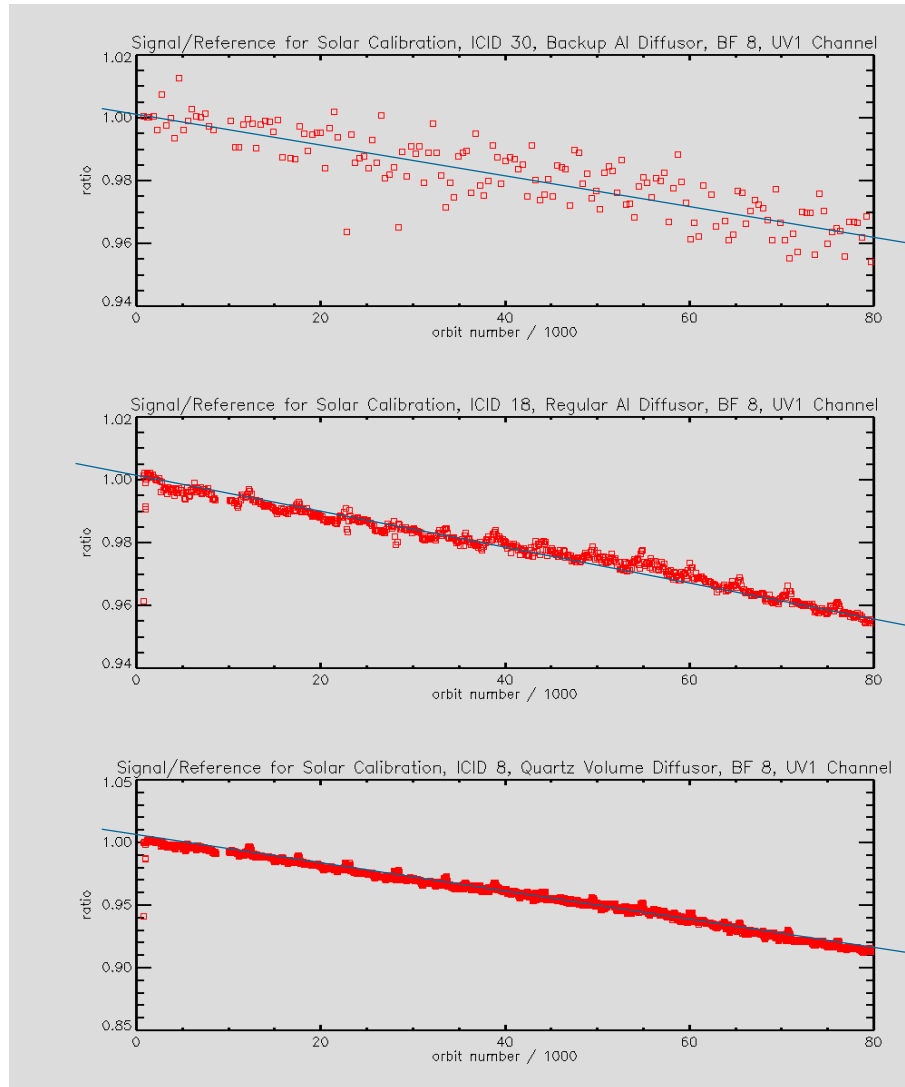
Optical stability is extremely good



Irradiance monitoring

Only UV1 shown

- QVD → daily
- ALU1 → weekly
- ALU2 → monthly
- Degradation includes :
 $D1 * FM * M2 * S * E$
- Exposure based degradation
- Backup ALU does not degrade
- Degradation may include electronic effects



2017	UV1	UV2	VIS
ALU2 monthly	0.97	0.975	0.975
ALU1 weekly	0.96	0.972	0.974
QVD daily	0.915	0.95	0.963
QVD path	8.5%	5.0%	3.7%
QVD only	5.5%	2.5%	1.2%
other inc FM	3.0%	2.5%	2.5%



Calibration Status: Wavelength calibration



Wavelength calibration monitoring

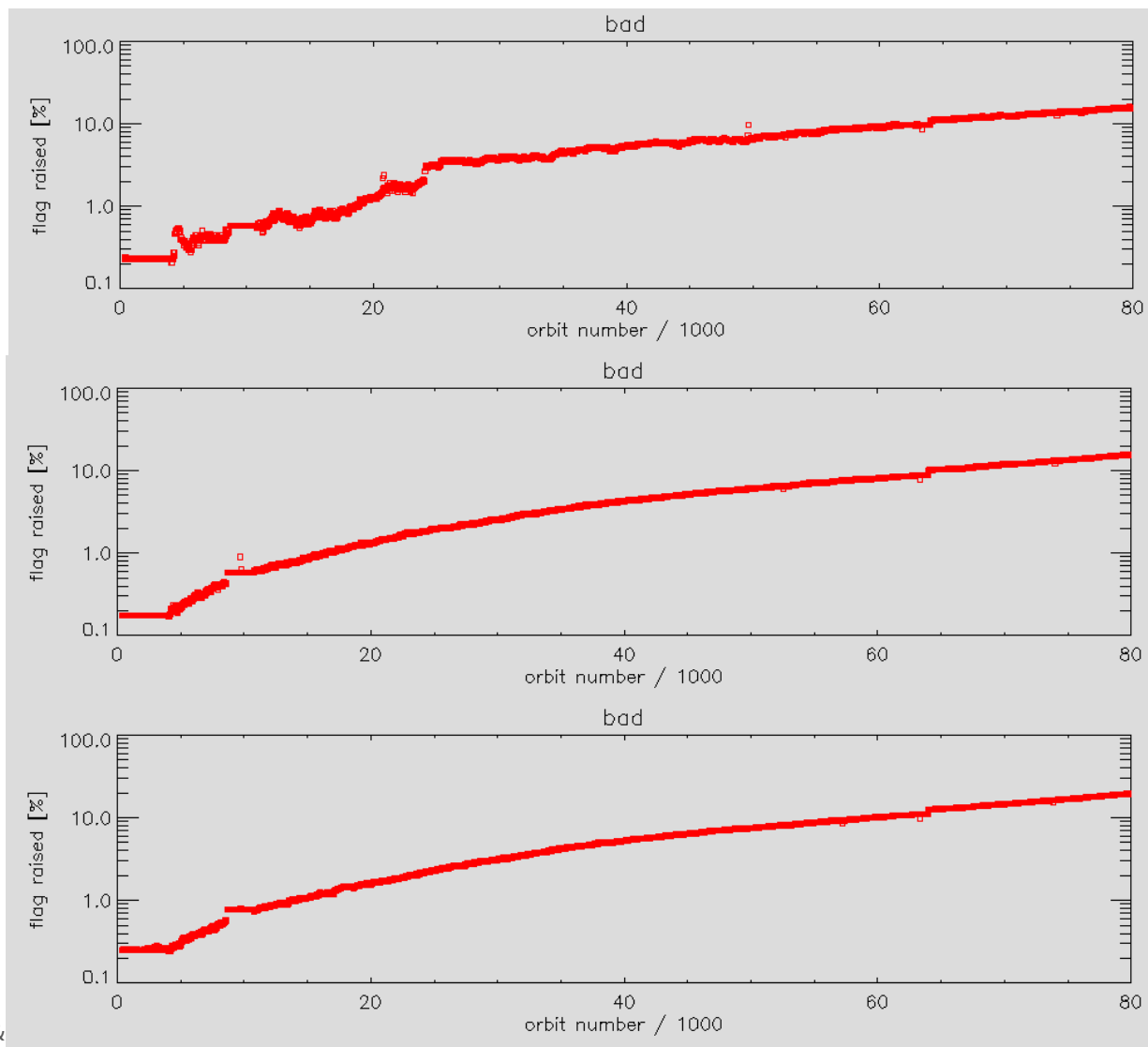
OMI's Spectral stability is very good

	UV1	UV2	VIS
trend	0.018 nm	0.000 nm	0.004 nm
seasonal [pp]	0.003 nm	0.004 nm	0.004 nm

Calibration Status Detector



CCD Detector Bad pixel monitoring



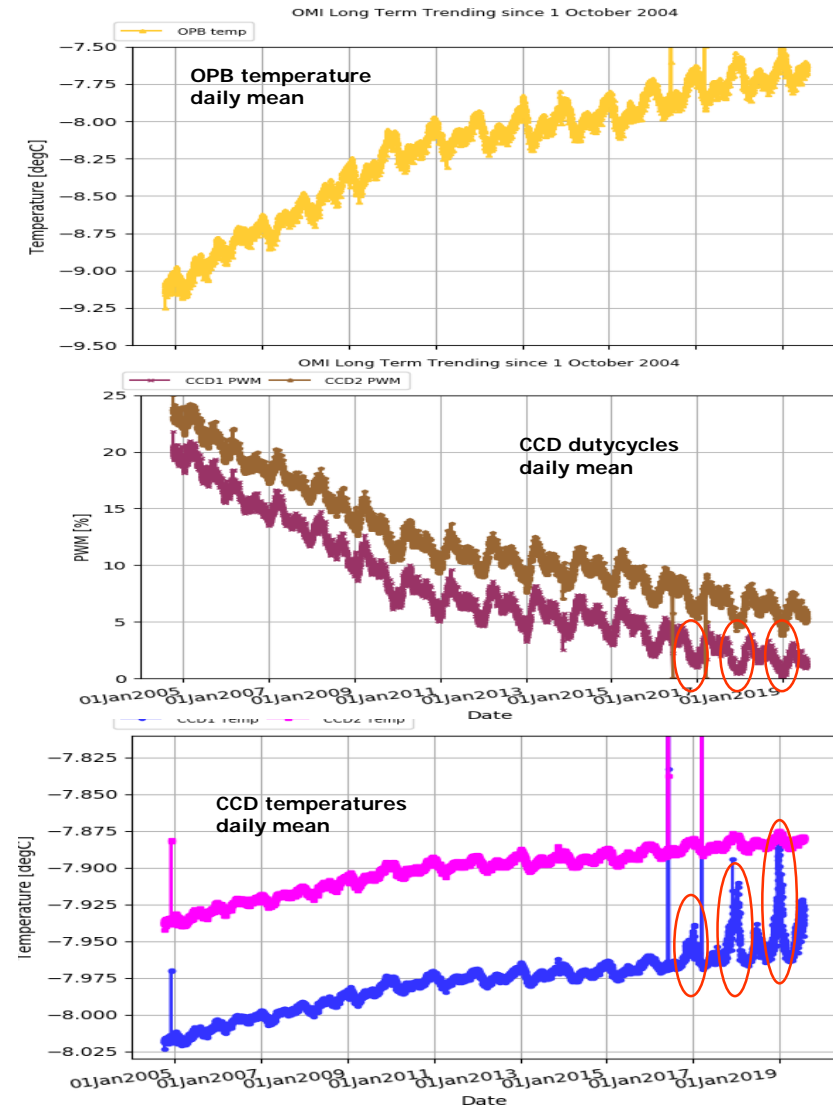
- Similar behavior for all three channels
- All channels above 10% bad pixels
- The bad flagging may be too aggressive
- Needs to be reconsidered in case of reprocessing.

OMI Operations & Calibration



❖ Temperatures

- Optical Bench (OPB) temperatures variation
 - orbit
 - seasonal
 - overall trend
- Degradation of cooler
 - Duty cycle of heaters decreases
- CCD temperatures
 - CCD2 (VIS) still stable
 - CCD1 (UV) unstable ~2 months per year
 - Effect on data negligible via a correction in the software





OMI Operations and level 1b

❖ Operations normal

- ❑ Save fuel: several options are discussed
- ❑ A-train discussions: decision this meeting is important for OMI due to impact on level 0-1b and operations

❖ Level 0-1b

- ❑ Recoding of the level 0-1b software (1 year effort, started recently)
 - for preparing for final collection 4 and reprocessing
 - This level 0-1b version includes new degradation corrections
 - Based on TROPOMI 0-1b processor, output compatible met TROPOMI
 - Interfaces simpler, 0-1b will fully run at NASA processor Centre

OMI Level 2 Product Updates KNMI

The KNMI OMI Level products will be updated based on the TROPOMI L2 processors.

- Algorithms will be updated based on the latest insights.
- Processors will support multi-threading.
- Native data format will be NetCDF4.
- Objective is to make OMI and TROPOMI L2 products compatible.

Data Product	Current OMI Processor	TROPOMI Processor
Cloud O ₂ -O ₂	OMCLDO2 v2	O22CLD
NO ₂	OMNO2A/DOMINO	S5P NO2 v2
Ozone Profile	OMO3PR v1	O3_PR v2
Aerosol	OMAERO v1	AER_AI v2, S5/S5P AOD
Ozone Column	OMDOAO3 v1	TBC

Product updates USA

- OMNO2 Version 4.0 release in 2019, major AMF updates [Lamsal et al., in prep.] :
 - Terrain reflectivity from a new MODIS-based geometry dependent Lambertian-equivalent reflectivity (GLER) product [Vasilkov et al., 2017; Qin et al., 2019; Fasnacht et al., 2019]
 - New cloud products incorporating GLER [Vasilkov et al., 2018]
 - Improved cloud & NO₂ retrievals over snow/ice surfaces
 - Detailed validation using ground-based (PANDORA, MxDOAS) and aircraft in-situ (P3B, DC-8) and remote sensing (GCAS, GEOTASO) observations [Choi et al., in prep.]
- OMAERUV products
 - AOD/SSA over ice & snow covered surfaces (OMI and MODIS combined use)
 - SSA over clouds for OMI/CALIOP collocated period (this product will in turn be used to calculate radiative forcing of aerosols above clouds)
- OMSO2 ongoing and future development
 - Data production ongoing for the latest OMI anthropogenic SO₂ product with improved Jacobian lookup table and enhanced retrievals over snow/ice. Release in ~1-2 months.
 - Implementation of efficient volcanic SO₂ height retrieval algorithm using machine learning
 - Improved SO₂ column retrievals over polluted regions using model-simulated daily *a priori* profiles and aerosol distribution.

Product updates USA (cont.)

- SAO products
 - OMHCHOd (level 3 gridded) released
 - Release new versions of HCHO (first half 2020) and H₂O, CHOCHO (second half 2020)
 - Release new version of ozone profile product with improved accuracy and long-term consistency next year.
- OMT03
 - October - OMT03 v9.0 public release with trend correction for degradation
 - Achieve long-term trend quality by calibrating with highly sensitive total ozone channels (302-306 nm) from OMI.
 - Understand differences in vertical & trend sensitivity in OMI and SBUV/MOD records.
 - Reduce errors from UV absorbing aerosols to improve accuracy of tropospheric ozone derived from OMT03-MLS differences.
 - Understand and attempt to mitigate effects of instrument aging on product quality (including effects on Raman cloud product).

Finland level 2: OMUVB status

- **Processing status:**

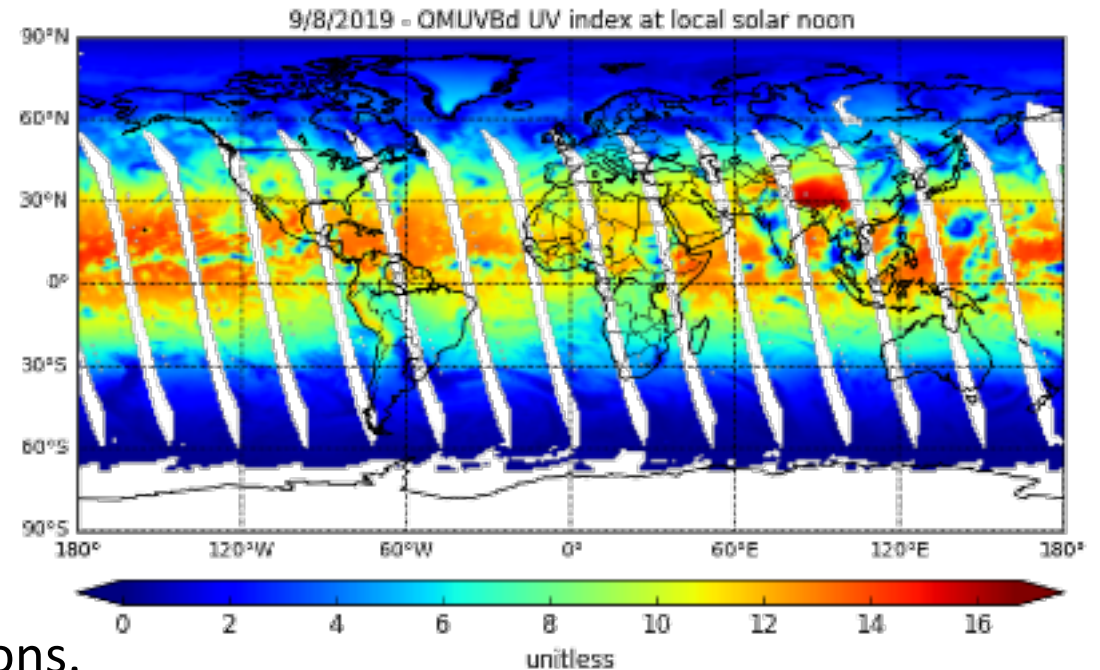
- FMI reprocessed OMUVB, OMUVBG and OMUVBd products in 2013 to include aerosol correction
- OMUVBG and OMUVBd were reprocessed again in 2016 after the PGEs were completely recoded in Python

- **Current versions:**

- OMUVB v1.3.1
- OMUVBG v2.0.0
- OMUVBd v2.0.0

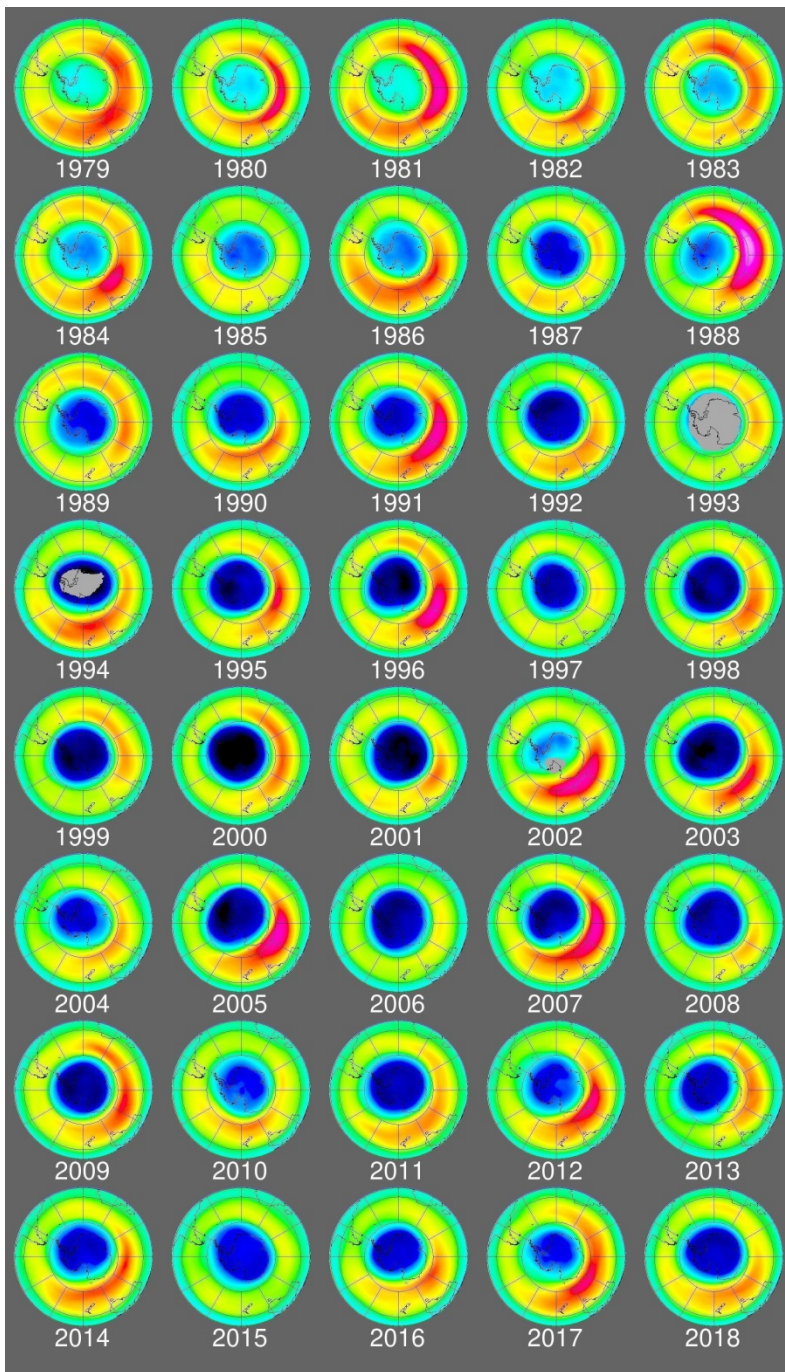
- **Data availability (10/2004 →):**

- FMI sftp server
- NASA Earthdata
- Users: health and environmental applications.
- <http://omi.fmi.fi>



Antarctic ozone hole

September average total ozone
KNMI Multi Sensor Reanalysis (MSR)
*incl. OMI total ozone, dominant/best
satellite source in MSR since 2004*

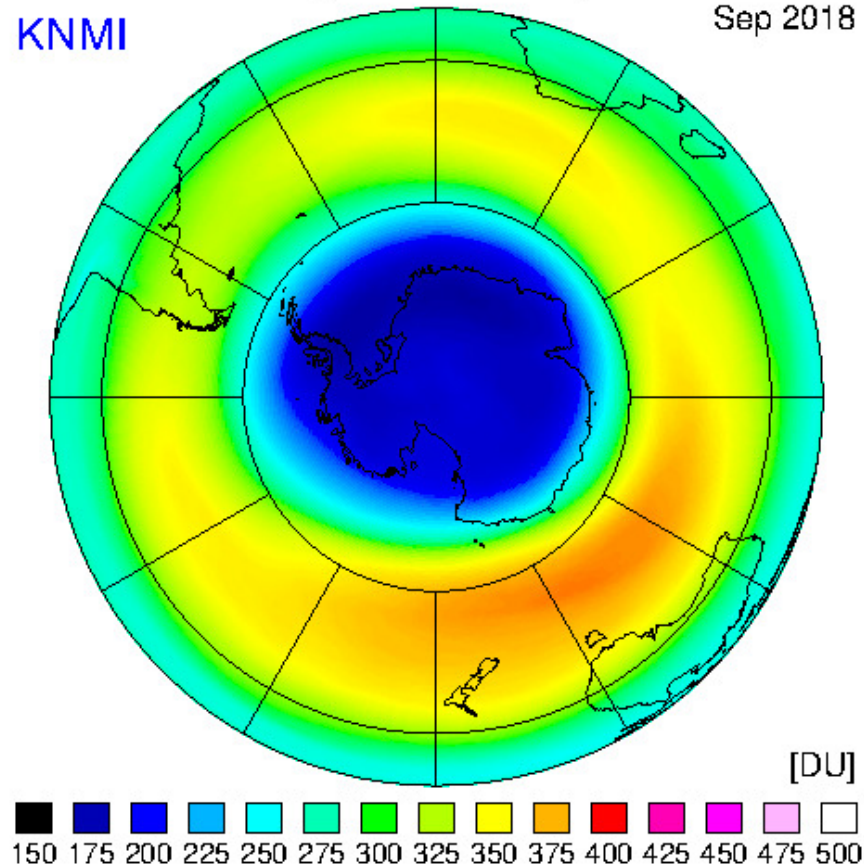


Multi Sensor Reanalysis 2

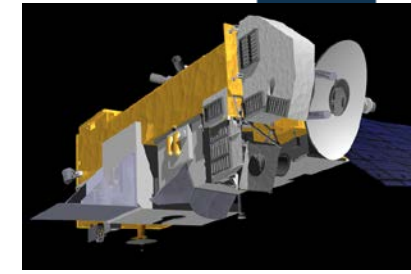
Monthly mean total ozone

KNMI

Sep 2018



Use of AURA observations in CAMS



Royal Netherlands
Meteorological Institute
Ministry of Infrastructure and the
Environment

CAMS: atmosphere.copernicus.eu

OMI and MLS satellite datasets are actively assimilated by CAMS

CAMS reanalysis, period 2003-2016 will soon be published (sep-oct 2018)

CAMS NRT analyses and forecasts
OMI O3 total column, NASA
MLS O3 profile NASA
OMI NO2 tropospheric column, KNMI
OMI SO2 column, NASA

CAMS reanalysis, based on:
OMI O3 total column, NASA
MLS O3 profile NASA
OMI NO2 tropospheric column, KNMI



SAMPO (OMI direct broadcast) dissemination via EUMETCast

Very Fast Delivery OMI and OMPS products produced as part of SAMPO service

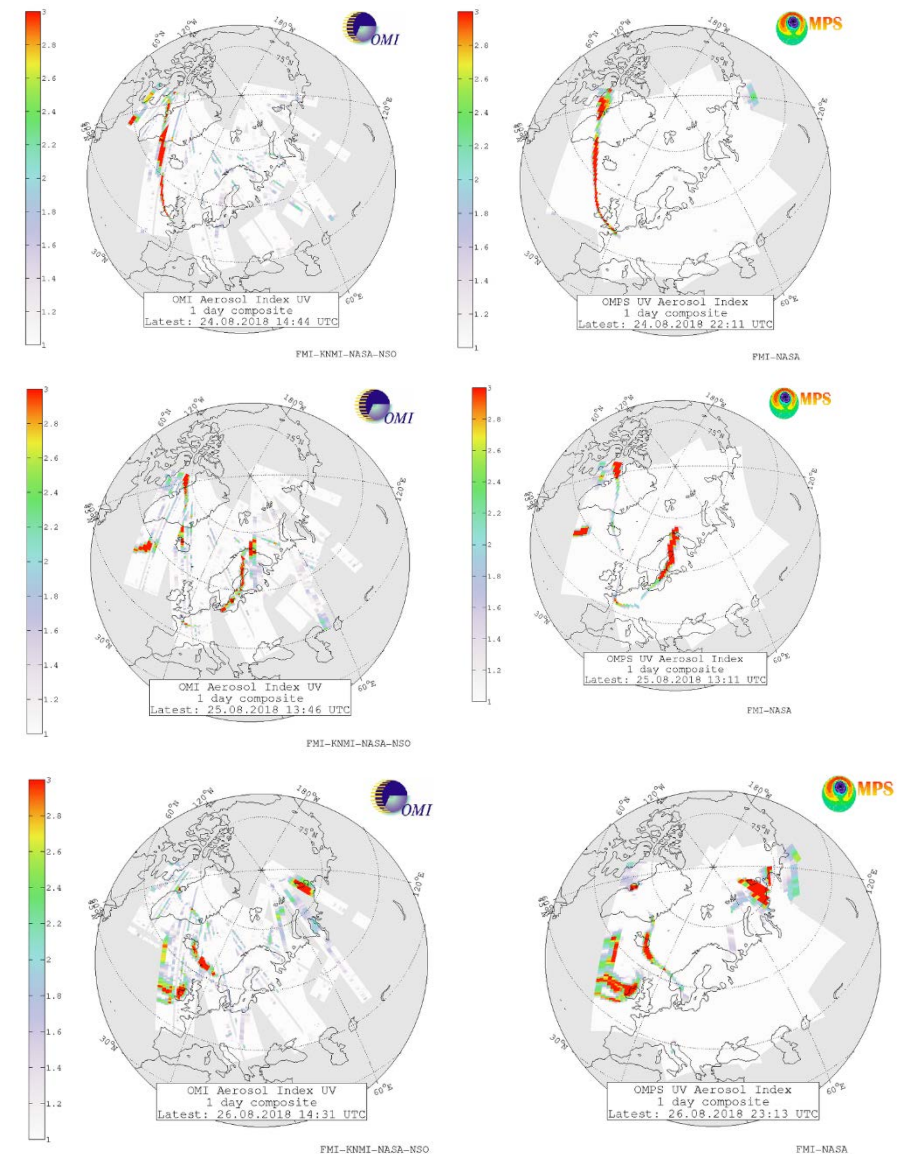
Service (sampo.fmi.fi)

- Maps available in 20 minutes
- Europe-Alaska-Arctic coverage

Monitoring

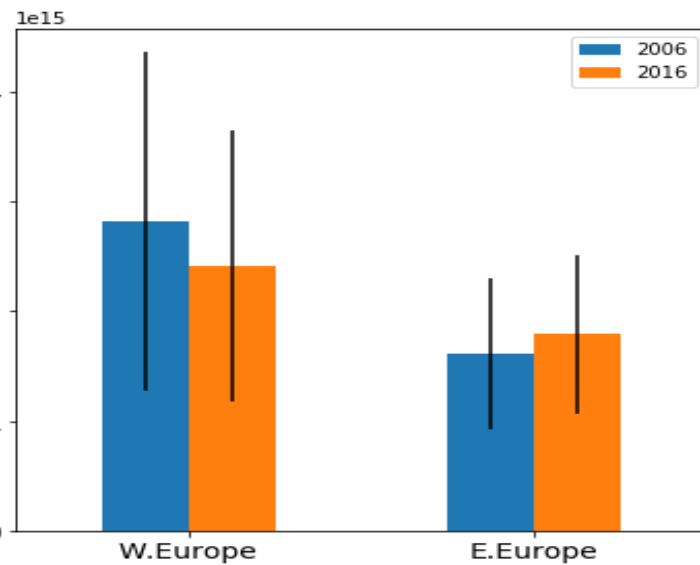
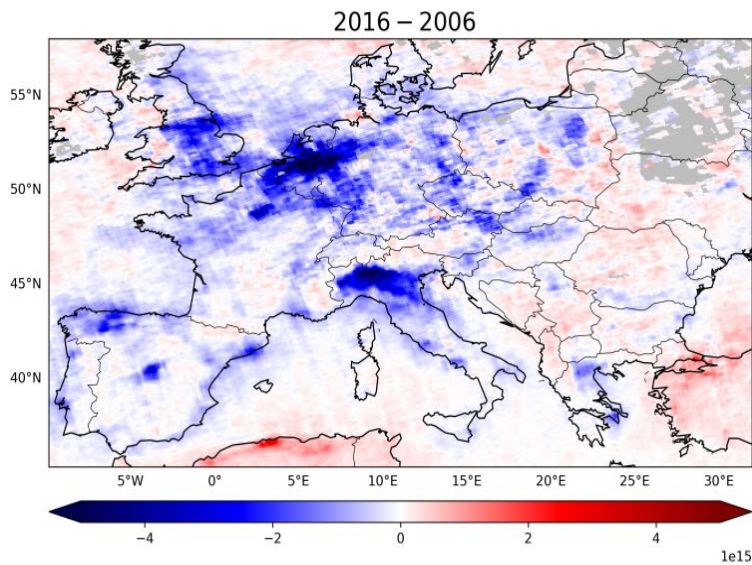
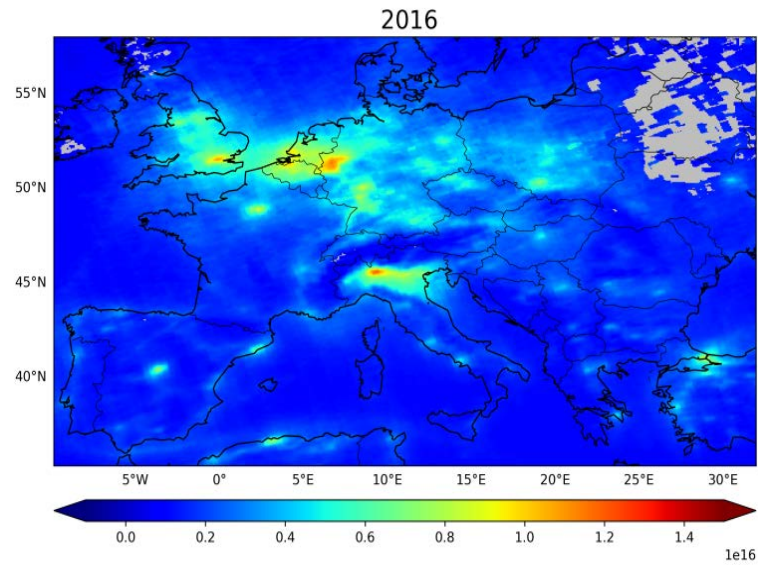
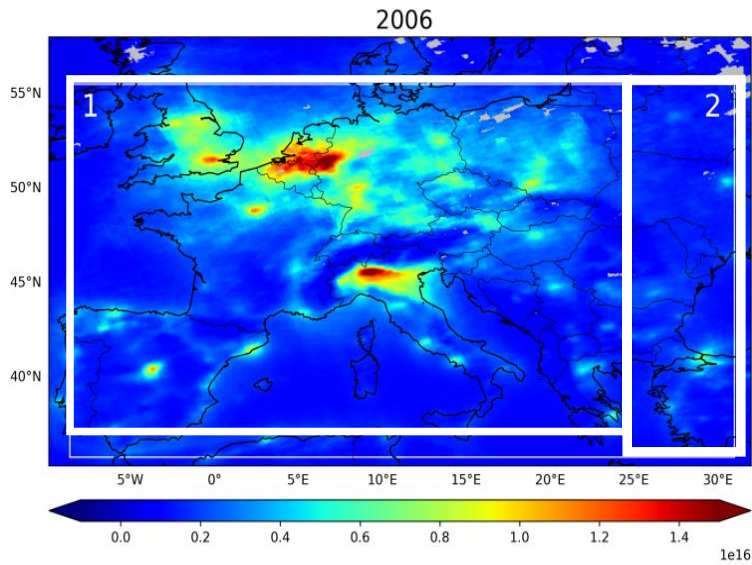
- Volcanic eruptions
- Ozone and ultraviolet radiation
- Forest fires

Data now also disseminated via EUMETCAST system



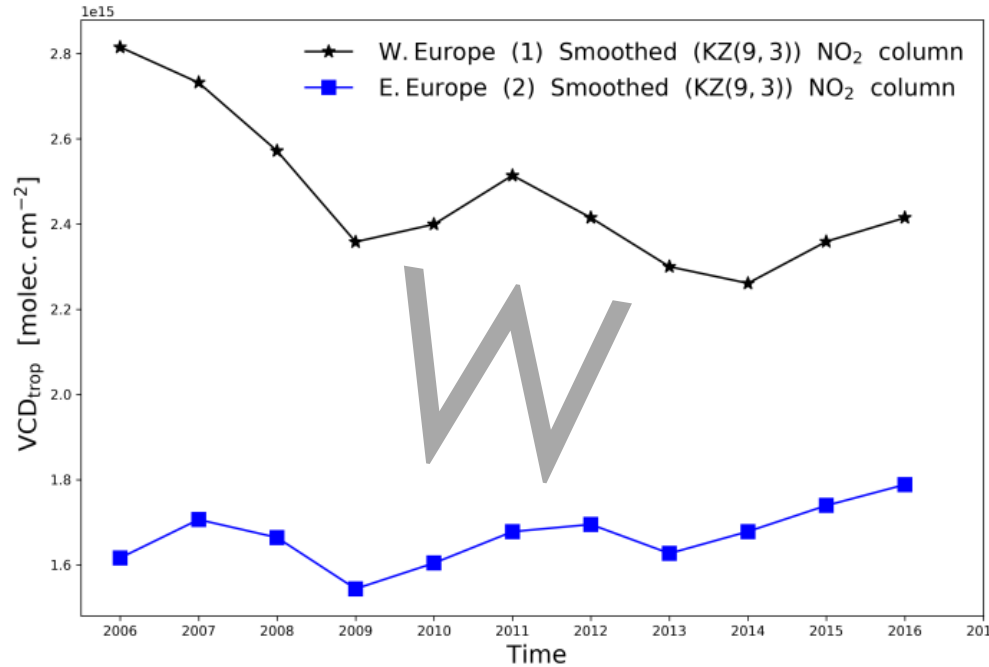
Smoke from Canadian forest fires reaching Europe, August 2018 (OMI and OMPS)

OMI record analyzed for trends over Europe

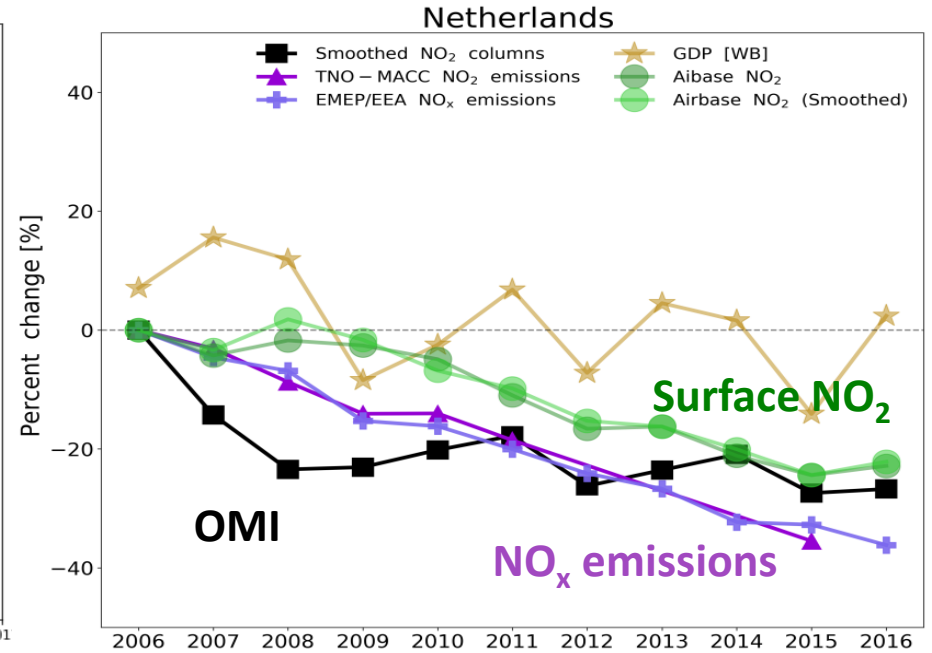


Western Europe (1): -14%
Eastern Europe (2): +11%

Column decrease has W-shape not apparent in surface NO₂



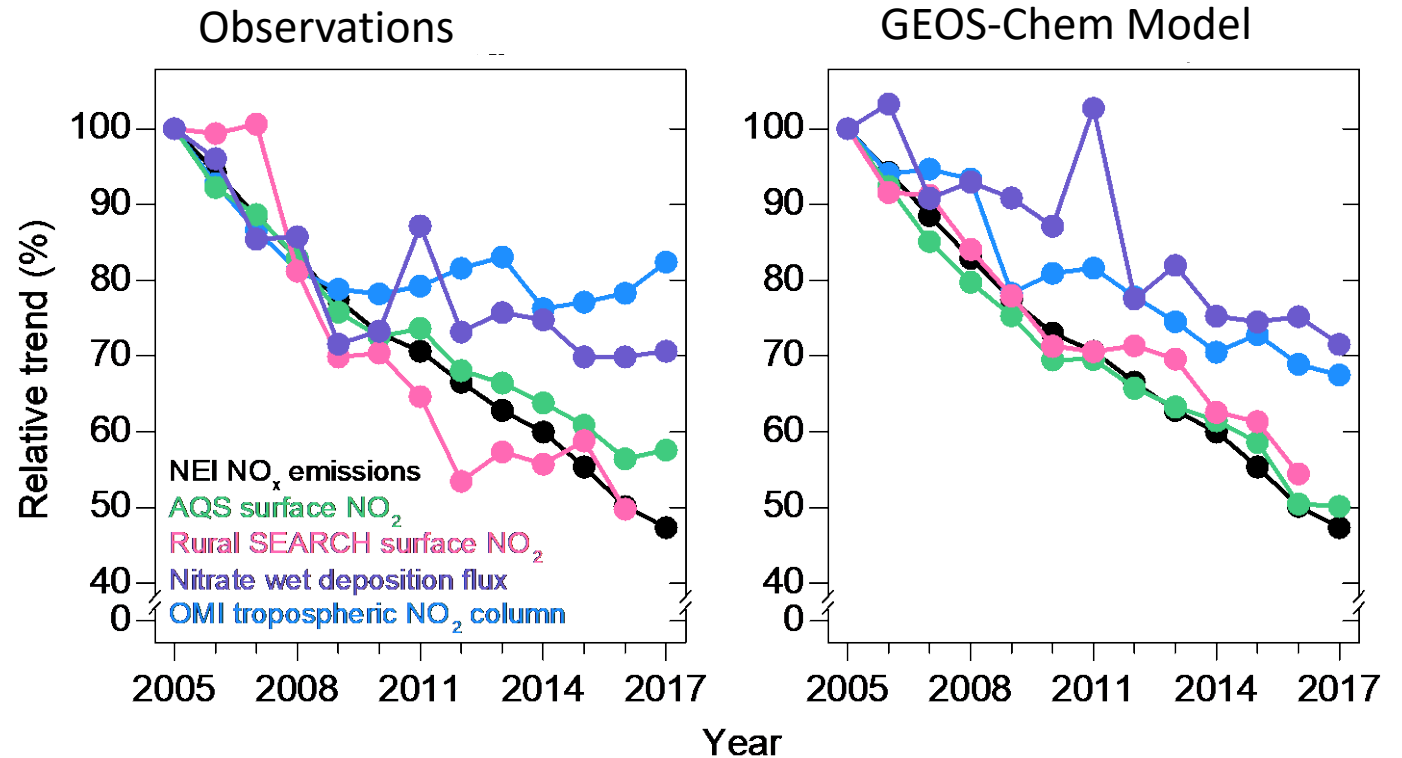
OMI NO₂ timeseries



OMI, surface, and emission timeseries

OMI tropospheric NO₂ columns used to infer long-term trends in US NO_x emissions: importance of accounting for the free-tropospheric NO₂ background

- The EPA's National Emission Inventory (NEI) reports a steady decrease of US NO_x emissions over 2005-2017
- OMI tropospheric NO₂ columns show steady decrease until 2009 and flattening afterward, previously attributed to a flattening of US NO_x emissions.

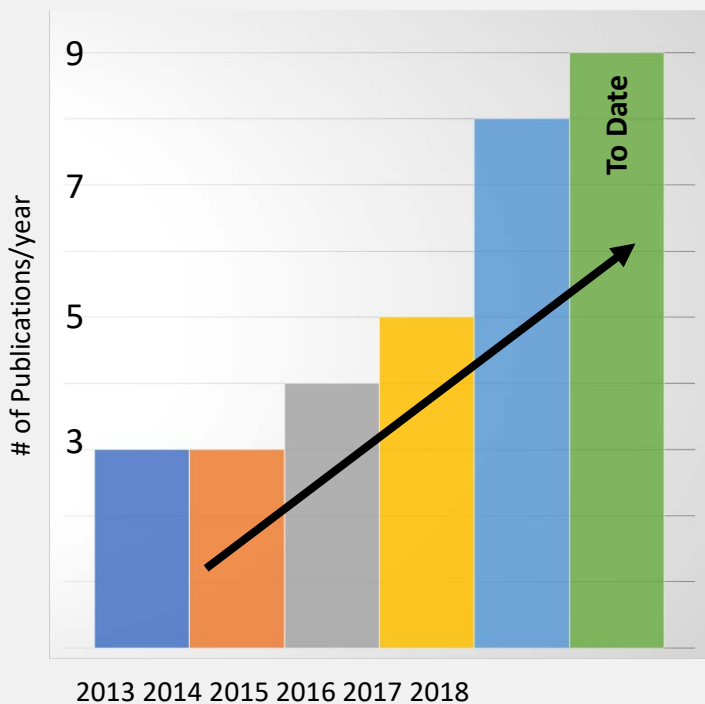


- Steady decrease of NEI NO_x emissions consistent with observed surface measurements and chemical transport modeling using GEOS-Chem.
- Post-2009 flattening of the OMI NO₂ trend is instead due to the increasing relative importance of the NO₂ background (from lightning and soil), rather than a flattening of US NO_x emissions.

Rising Use of Aura OMI Products for Health Exposure Assessments

- The use of Aura OMI products has increased in health risk studies in the last 5 years for:
 - (1) UV radiation exposure (i.e., Aerosol, O₃, surface albedo)
 - (2) Air pollutant exposure (i.e., NO₂, CH₂O)
- Applications of OMI data are wide-spread including: Australia, China, Canada, Europe, South America, and the US.

Health Exposure Publications Using Aura OMI Data



Via Google Scholar & Web of Science

ENVIRONMENTAL Science & Technology

Cite This: *Environ. Sci. Technol.* 2018, 52, 4180–4189

Article
pubs.acs.org/est

Satellite-Based Estimates of Daily NO₂ Exposure in China Using Hybrid Random Forest and Spatiotemporal Kriging Model

Yu Zhan,^{†,‡,§} Yuzhou Luo,^{||} Xunfei Deng,[⊥] Kaishan Zhang,[†] Minghua Zhang,^{||} Michael L. Grieneisen,^{||} and Baofeng Di^{*,†,‡,§}

[†]Department of Environmental Science and Engineering, Sichuan University, Chengdu, Sichuan 610065, China
[‡]Institute for Disaster Management and Reconstruction, Sichuan University, Chengdu, Sichuan 610200, China
[§]Sino-German Centre for Water and Health Research, Sichuan University, Chengdu, Sichuan 610065, China
^{||}Department of Land, Air, and Water Resources, University of California, Davis, California 95616, United States
[⊥]Institute of Digital Agriculture, Zhejiang Academy of Agricultural Sciences, Hangzhou, Zhejiang 310021, China

Supporting Information

ABSTRACT: A novel model named random-forest-spatiotemporal-kriging (RF-STK) was developed to estimate the daily ambient NO₂ concentrations across China during 2013–2016 based on the satellite retrievals and geographic covariates. The RF-STK model showed good prediction performance, with cross-validation R² = 0.62 (RMSE = 13.3 μg/m³) for daily and R² = 0.73 (RMSE = 6.5 μg/m³) for spatial predictions. The nationwide population-weighted multyear average of NO₂ was predicted to be 30.9 ± 11.7 μg/m³ (mean ± standard deviation), with a slowly but significantly decreasing trend at a rate of -0.88 ± 0.38 μg/m³/year. Among the main economic zones of China, the Pearl River Delta showed the fastest decreasing rate of -1.37 μg/m³/year, while the Beijing-Tianjin Metro did not show a temporal trend (P = 0.32). The population-weighted NO₂ was predicted to be the highest in North China (40.3 ± 10.3 μg/m³) and lowest in Southwest China (24.9 ± 9.4 μg/m³). Approximately 25% of the population lived in nonattainment areas with annual-average NO₂ > 40 μg/m³. A piecewise linear function with an abrupt point around 100 people/km² characterized the relationship between the population density and the NO₂, indicating a threshold of aggravated NO₂ pollution due to urbanization. Leveraging the ground-level NO₂ observations, this study fills the gap of statistically modeling

Environmental Big Data → Machine Learning Geostatistics → Surface NO₂

Environment International 120 (2018) 81–92

Contents lists available at ScienceDirect

Environment International

journal homepage: www.elsevier.com/locate/envint

Spatial PM_{2.5}, NO₂, O₃ and BC models for Western Europe – Evaluation of spatiotemporal stability

Kees de Hoogh^{a,b,*}, Jie Chen^c, John Gulliver^d, Barbara Hoffmann^e, Ole Hertel^f, Matthias Ketzel^f, Mariska Bauwelinck^{g,h}, Aaron van Donkelaarⁱ, Ulla A. Hvidtfeldt^j, Klea Katsouyanni^{k,l}, Jochem Klompmaker^{m,n}, Randal V. Martin^{h,o}, Evangelia Samoli^h, Per E. Schwartz^o, Massimo Stafoggia^{p,q}, Tom Bellander^q, Maciej Strak^r, Kathrin Wolf^r, Danielle Vienneau^{u,v}, Bert Brunekreef^{c,s}, Gerard Hoek^c

Air Quality, Atmosphere & Health (2018) 11:755–764
<https://doi.org/10.1007/s11869-018-0582-4>

Ambient air pollution and the prevalence of rhinoconjunctivitis in adolescents: a worldwide ecological analysis

Barbara K. Butland¹ · H. Ross Anderson^{1,2} · Aaron van Donkelaar³ · Elaine Fuentes⁴ · Michael Brauer⁵ · Bert Brunekreef^{6,7} · Randall V. Martin^{3,8} · the ISAAC Phase Three Study Group

Received: 28 February 2017 / Accepted: 30 April 2018 / Published online: 23 June 2018
 © The Author(s) 2018

Abstract
 Whether exposure to outdoor air pollution increases the prevalence of rhinoconjunctivitis in children is unclear. Using Three of the International Study of Asthma and Allergies in childhood (ISAAC), we investigated associations of prevalence in adolescents with model-based estimates of ozone, and satellite-based estimates of fine (diameter < 2.5 μm) particulate matter (PM_{2.5}).

From the journal:
Photochemical & Photobiological Sciences

The geospatial relationship of pterygium and senile cataract with ambient solar ultraviolet in tropical Ecuador

Daniel R. Garzón-Chavez,^{abc} Emmanuelle Quentin,^d Simone L. Harrison,^{bc} Alfio V. Parisi,^{cb} Harry J. Butler^c and Nathan J. Downs^{*cb}

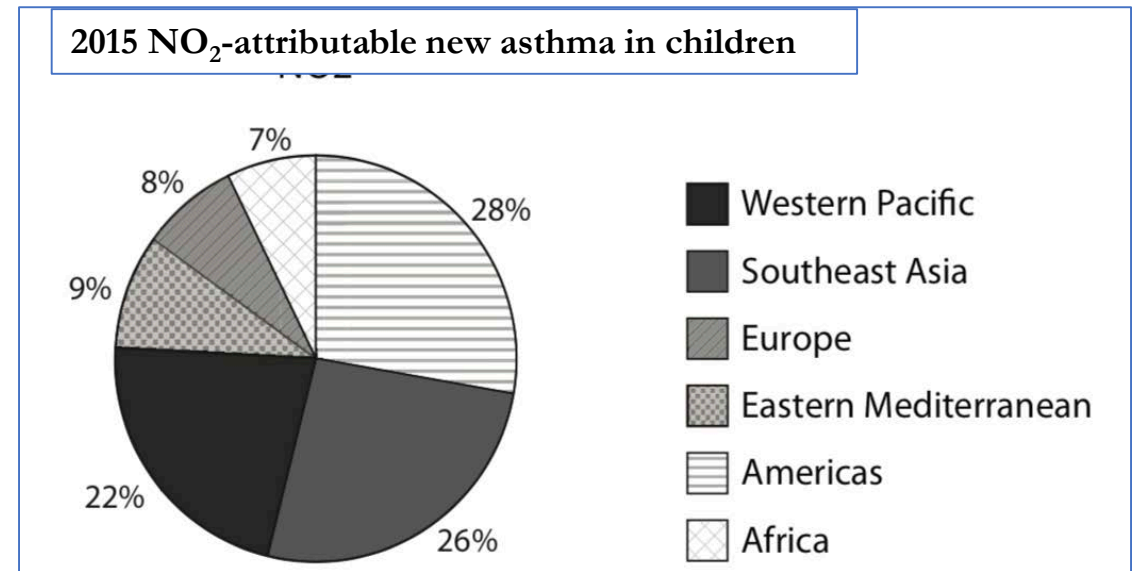
Author affiliations

Abstract

Tropical Ecuador presents a unique climate in which we study the relationship between the ambient levels of solar ultraviolet radiation and eye disease in the absence of a latitudinal gradient. The national distribution of surface ultraviolet, taking into account MODIS and OMI satellite observation of aerosol, ozone, surface albedo, local elevation and cloud fractions measured during 2011, was compared with the national pterygium (WHO ICD H11) and senile cataract (WHO ICD H25) incidence projected from the 2010 National Institute of Statistics and Census (Ecuador). Public Health Ministry projections for age categories 0 to 39, 40 to 59 and 60+ years were compared to surface ultraviolet irradiance data in 1040 parishes. Correlations drawn between modelled surface

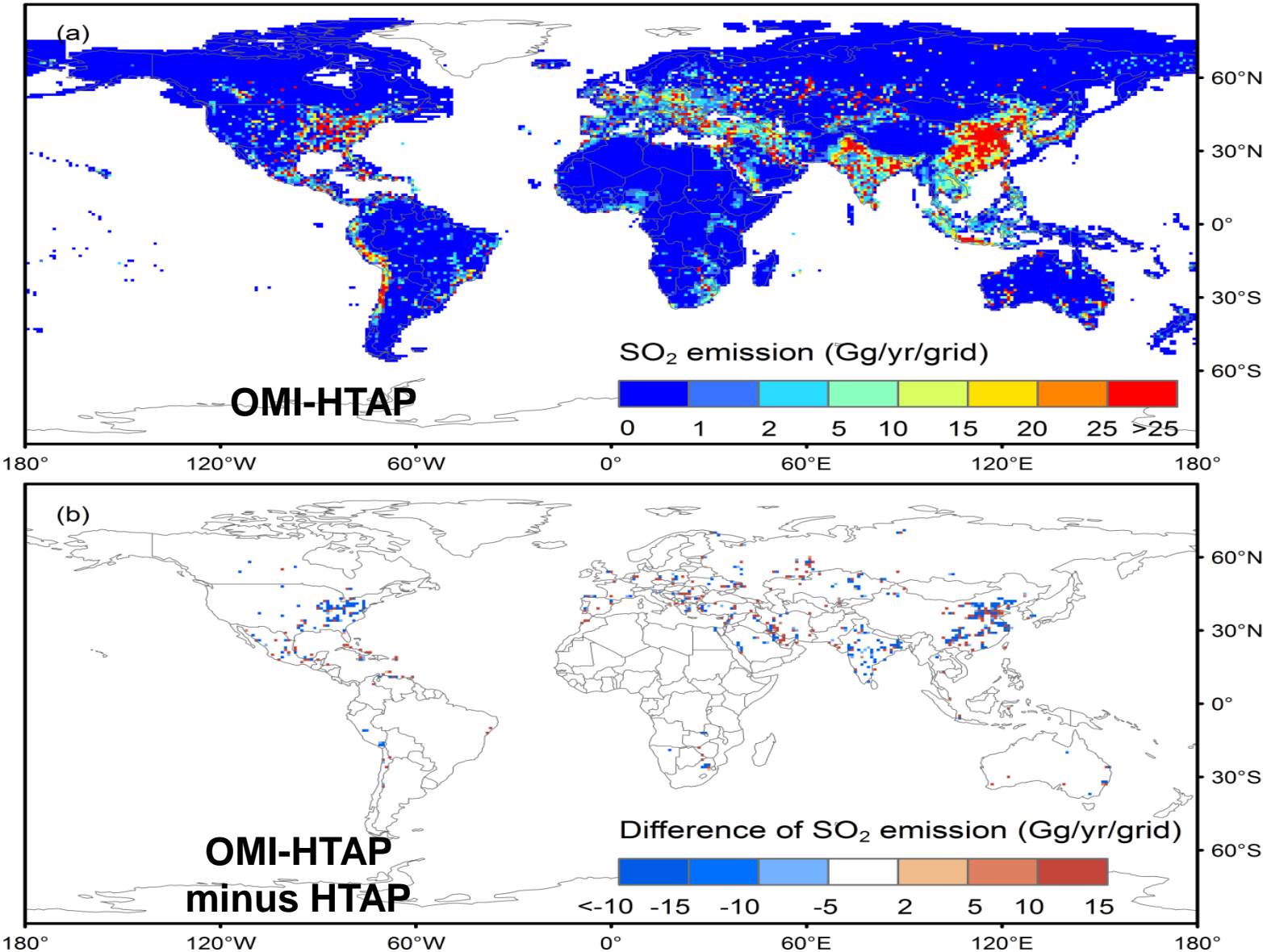
Application of OMI NO₂ to estimate surface NO₂ effect globally on asthma exacerbation and incidence

- Adverse asthma health effects may be attributable to air pollutants including NO₂
- First estimates of the global asthma burden from ambient air pollution used OMI and other pollution data sets, epidemiologically derived health-impact functions, population datasets (NASA SEDAC), and baseline asthma statistics.



- Up to ~1 million new pediatric asthma cases could occur globally due to anthropogenic NO₂, including the Americas with ~28% of new cases.
- The relatively coarse resolution of OMI data may underestimate the asthma burden in the present study. Follow-on work will examine the use of more finely-resolved TROPOMI NO₂ data.

New global SO₂ emission inventory OMI-HTAP



A new global anthropogenic SO₂ emission inventory OMI-HTAP based on both satellite-derived and bottom-up emissions

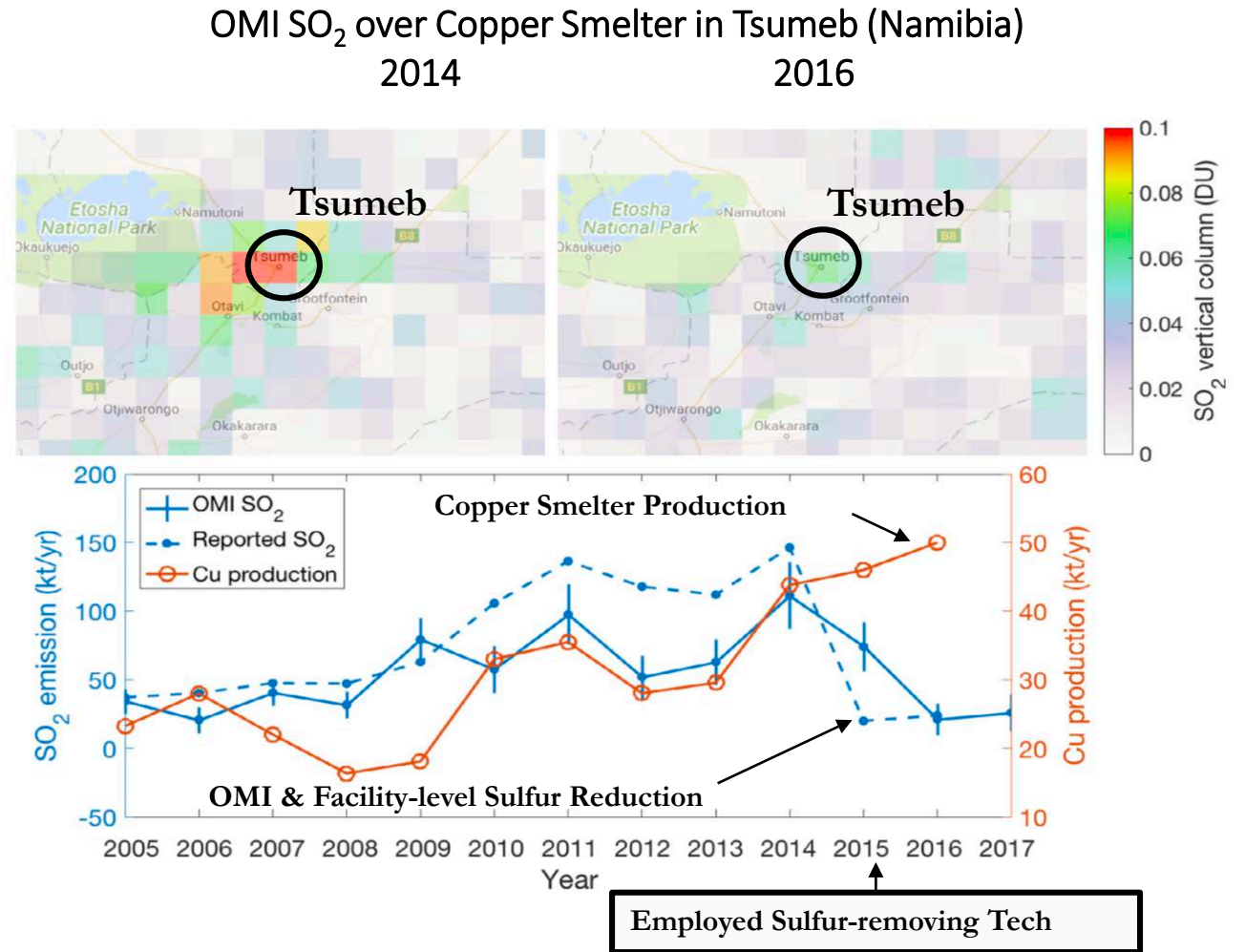
- Add missing sources detected by OMI: higher values over Middle East, Mexico and Russia
- Correct misallocations of large point sources

GEOS-5 simulating SO₂ shows better agreement with in-situ measurements when driven by OMI-HTAP

Liu, F., Choi, S., Li, C., Fioletov, V. E., McLinden, C. A., Joiner, J., Krotkov, N. A., Bian, H., Janssens-Maenhout, G., Darmenov, A. S., and da Silva, A. M.: A new global anthropogenic SO₂ emission inventory for the last decade: A mosaic of satellite-derived and bottom-up emissions, *Atmos. Chem. Phys. Discuss.*, <https://doi.org/10.5194/acp-2018-331>, in review, 2018.

OMI: Application of Aura OMI SO₂ Observations Supporting the Cleantech Industry's Goal of Reducing Air Pollution

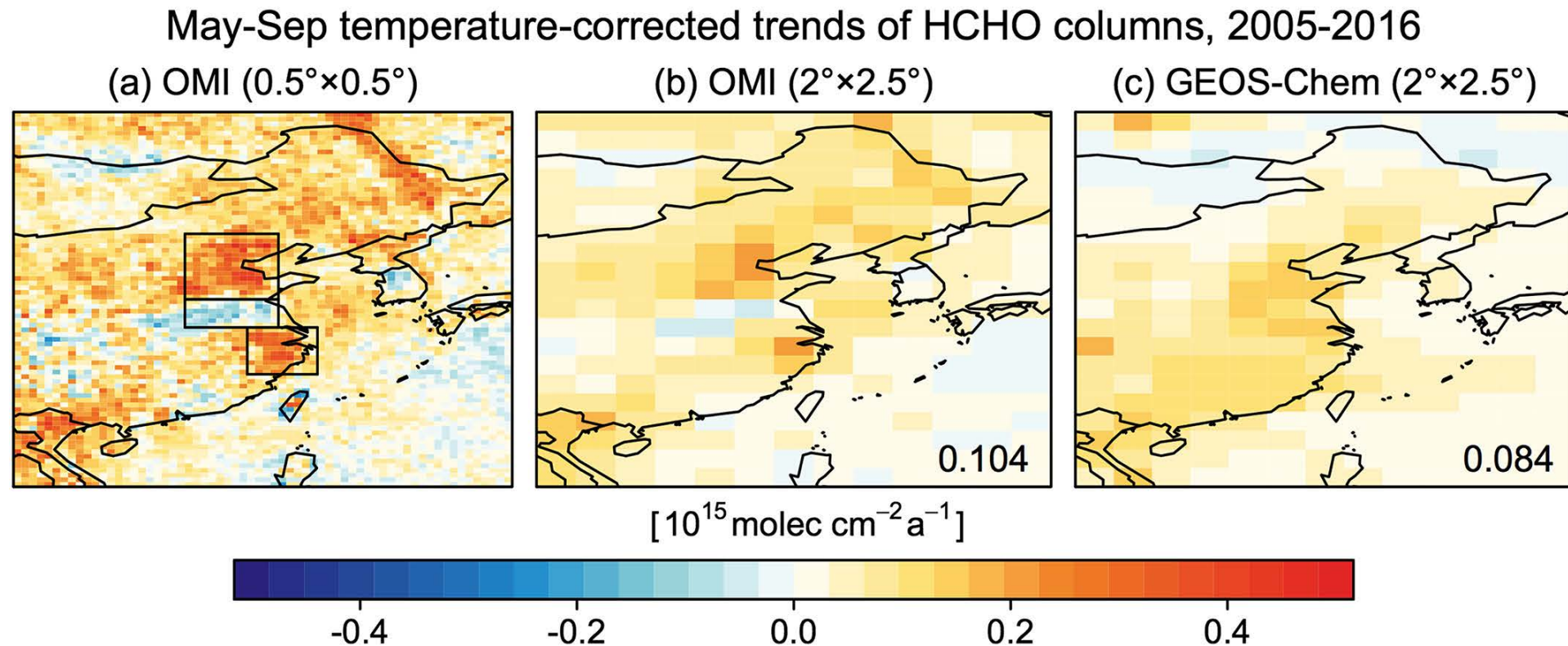
- Aura OMI-based observations can support industry and prove the efficacy of cleantech solutions in reducing air pollution.
- A large reduction (about 80%) in SO₂ emissions was observed **by OMI** after the implementation of a sulfur-capture plant (designed to remove SO₂ emissions to air) at the smelter by Finnish cleantech company, Outotec Oy, in 2015.
- Space-based (**OMI SO₂**) and facility-level (**reported SO₂**) emissions capture similar temporal variability.
- ~90% decrease in SO₂ emissions, also found at copper smelter in Bor, Serbia, where Outotec Oy also installed a sulfur-capture plant.



Ialongo, et al., *Environ. Tech. & Innov.*, 2018.

2005-2016 trends of formaldehyde columns over China observed by satellites: increasing anthropogenic emissions of volatile organic compounds and decreasing agricultural fire emissions

Shen et al., GRL, 46, 8, <https://doi.org/10.1029/2019GL082172>

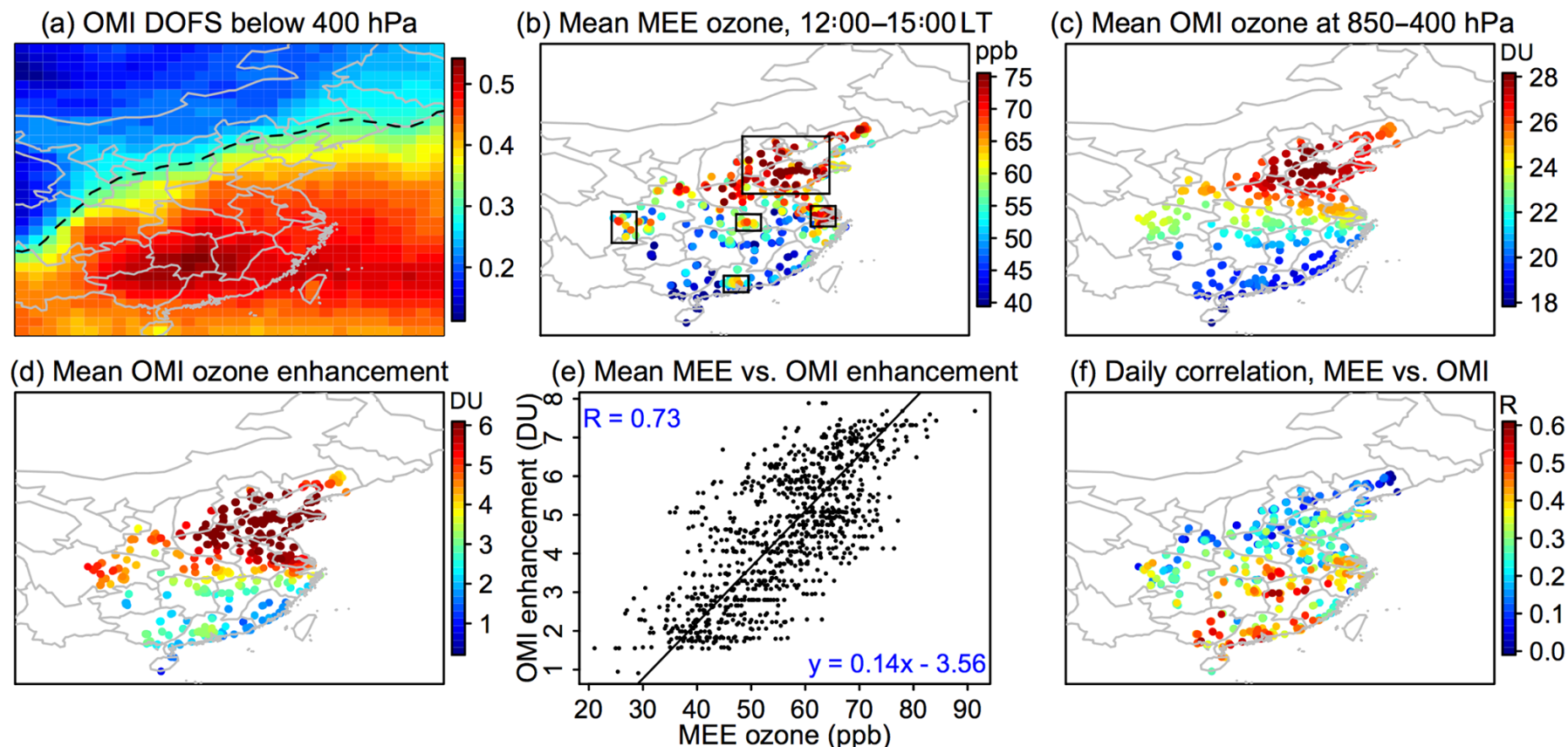


The 2005–2016 trends of formaldehyde columns over China. Values are fitted linear trends for May–September 5-month averages of each year. OMI trends are corrected for temperature. (a) Observed OMI trends on the $0.5^\circ \times 0.5^\circ$ grid. From top to bottom, the three rectangles delineate the North China Plain, Huai River Basin, and Yangtze River Delta. (b) Same as (a) but on a $2^\circ \times 2.5^\circ$ grid. (c) 2005–2016 trends simulated by GEOS-Chem at $2^\circ \times 2.5^\circ$ resolution with fixed biogenic sources at the 2005 level. The averaged trends in eastern China are shown inset.

Tropospheric ozone : Spatial distribution and temporal trends of Ozone pollution in China observed with OMI (SAO OMPROFOZ), 2005-2017

Shen et al., ACP, 19, 6551-6560, <https://doi.org/10.5194/acp-19-6551-2019>

Summer (JJA) 2013–2017 ozone over China from the MEE network and the OMI instrument

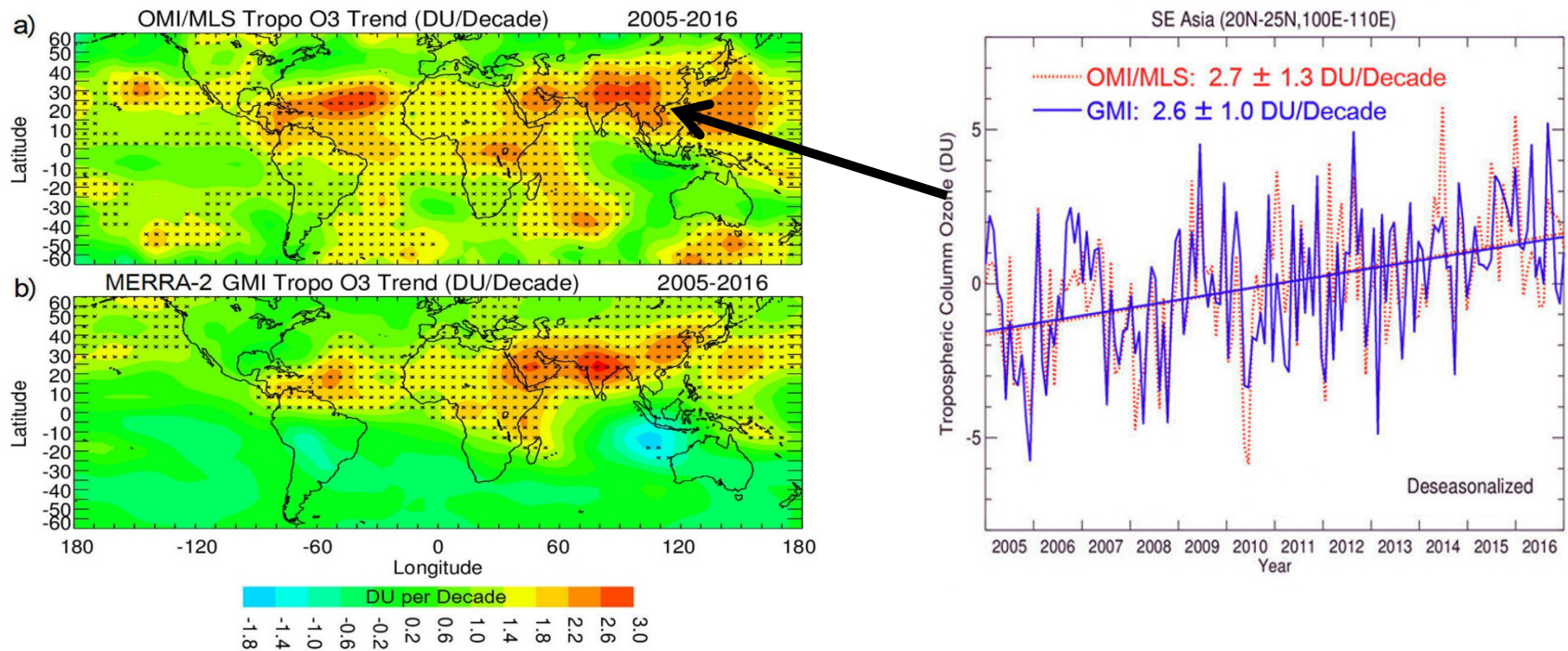


Summertime observations of O_3 over China (JJA 2013–2017) from the MEE surface network and OMI. (a) Mean degrees of freedom for signal (DOFS) of SAO OMPROFOZ O_3 retrievals (Liu et al. 2010) below 400 hPa. We limit our attention to the China domain with DOFS>0.3 and to sites with at least 100 concurrent surface and OMI observations during 2013–2017. (b) Mean midday (12–15 local time) O_3 from the MEE surface network. Rectangles identify high- O_3 regions discussed in the text including Beijing–Tianjin–Hebei (BTH, 114–121 E and 34–41 E), Yangtze River Delta (YRD, 119.5–121.5 E and 30–32.5 E), Pearl River Delta (PRD, 112.5–114.5 E and 22–24 E), Sichuan Basin (SCB, 103.5–105.5 E and 28–31.5 E) and Wuhan (113.5–115.5 E and 29.5–31.5 E). (c) Mean OMI partial columns at 850–400 hPa. (d) Mean OMI O_3 enhancements at 850–400 hPa after subtraction of the latitude-dependent mean background over the Pacific (150 E–150 W). (e) Spatial correlation of mean JJA 2013–2017 MEE O_3 with OMI O_3 enhancement at 850–400 hPa. (f) Temporal correlation coefficients (R) of daily MEE surface O_3 with OMI at individual sites measuring the ability of OMI to capture the day-to-day variability of surface O_3 .

Tropospheric Ozone: Trends in global tropospheric ozone inferred from OMI & MLS and the MERRA-2 GMI simulation

OMI/MLS satellite measurements identify increases in tropospheric ozone over Saudi Arabia, India, SE Asia, and other regions

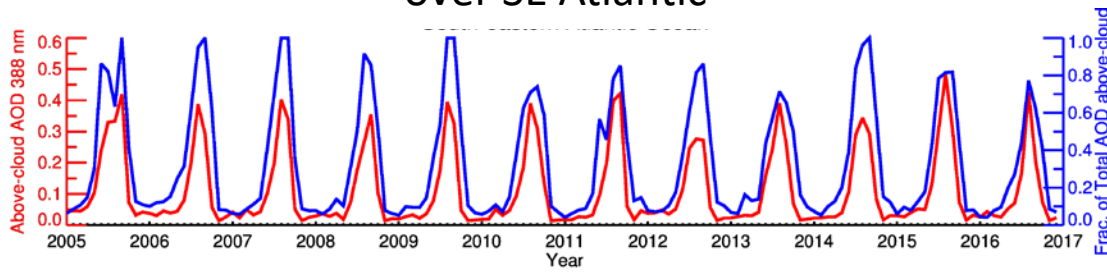
GMI model simulation indicates that tropospheric ozone increases over Saudi Arabia, India, SE Asia are due to increases in pollution



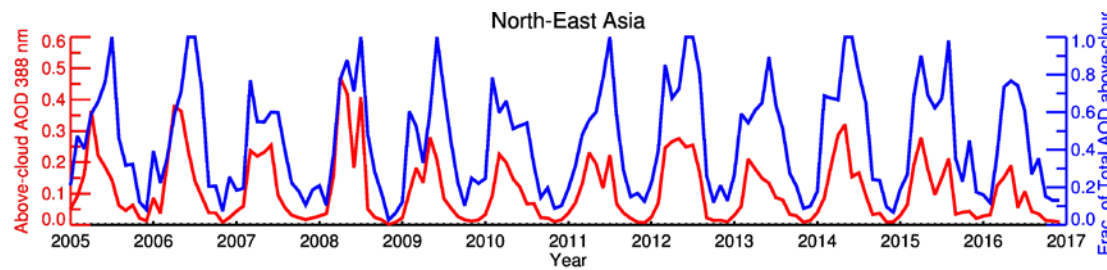
OMI climate data set: 12-year global record of absorbing aerosol optical depth over cloud

Implications for aerosol-cloud radiation interaction studies

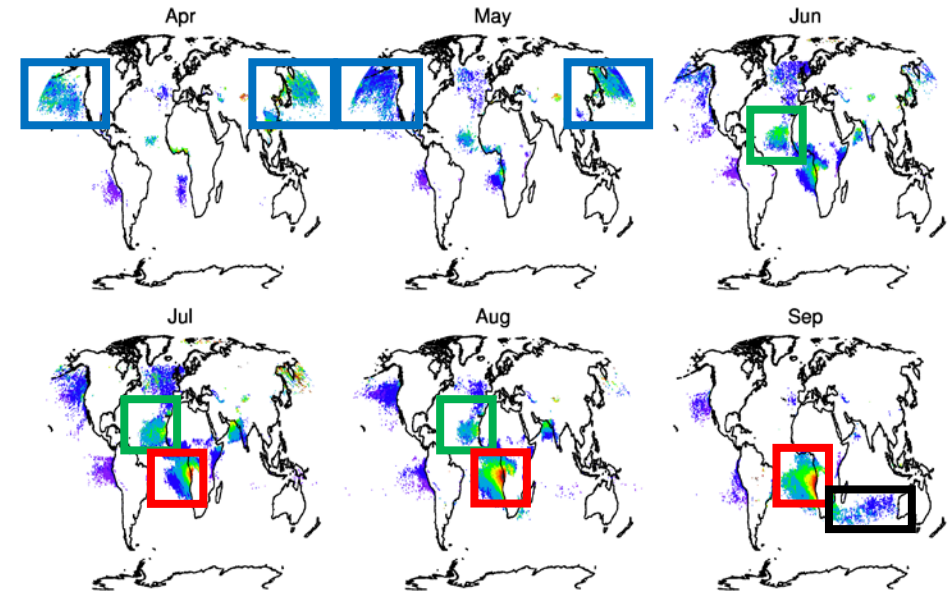
No significant temporal trend in above-cloud AOD over SE Atlantic



Negative temporal trend over NE Asia- prominent decrease 2009 onwards



12-year monthly climatology of OMI above-cloud aerosol optical depth



Blue box: Trans-Pacific transport of dust and pollution over clouds

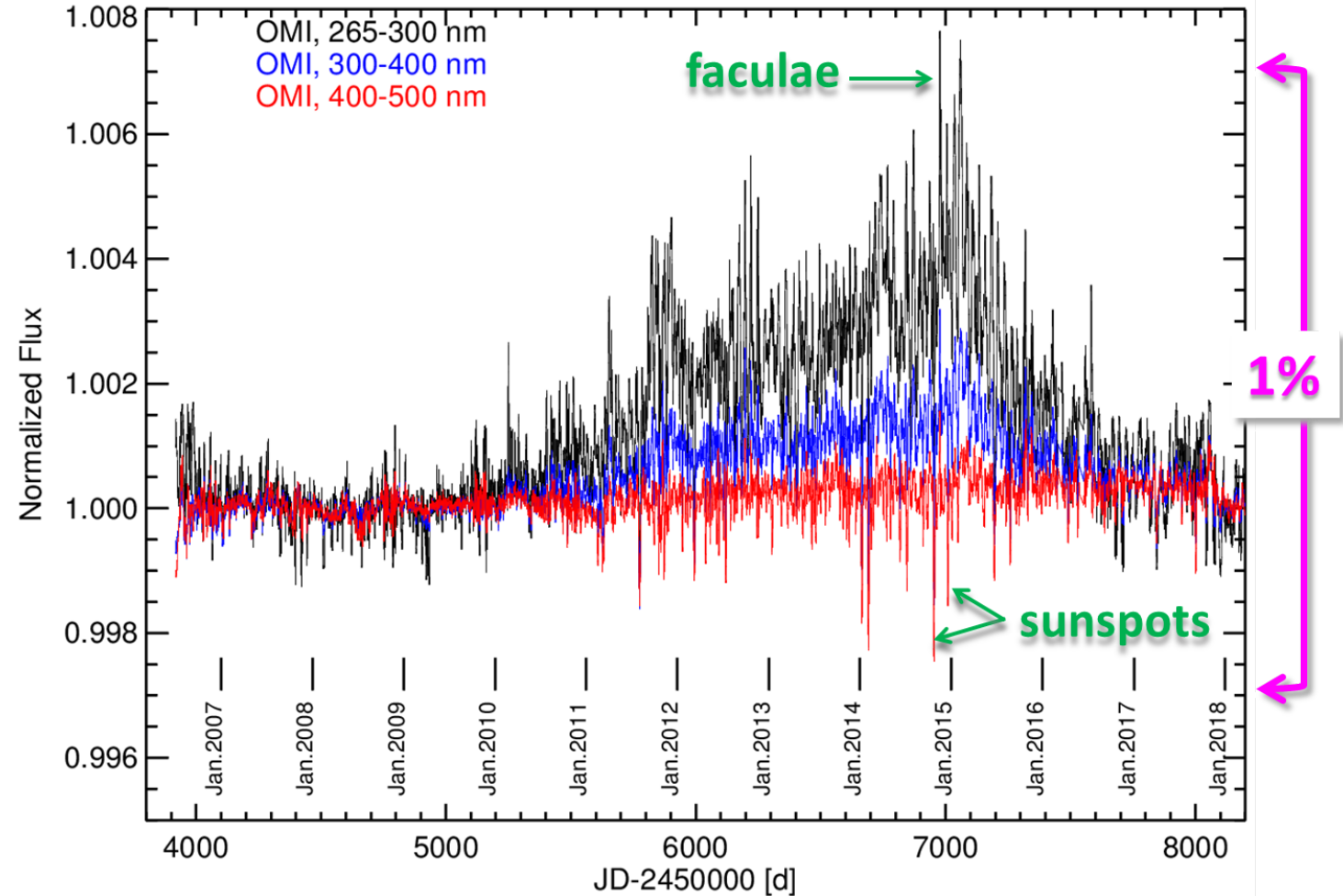
Green box: Saharan dust transport over tropical Atlantic

Red box: Transport of African smoke above clouds over SE Atlantic

Black box: Trans-Indian Ocean transport of southern African smoke above clouds along the sub-tropical jet

OMI Solar Spectral Irradiance (SSI)

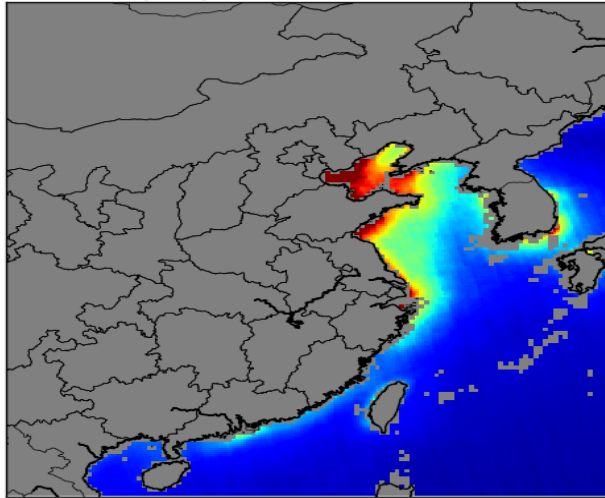
- OMI's unprecedented stability and characterization has made it a standard for UV/Vis SSI measurements
- OMI SSI data set (2006-2018) now covers full range of solar cycle 24
- Short-term solar variability (bright faculae, dark sunspots) clearly seen with high precision
- Long-term uncertainty (0.1% in UV, 0.05% in visible)
- OMI data being used to validate SSI models (e.g. NRLSSI2)



Marchenko et al., *Earth and Space Science*, in review.

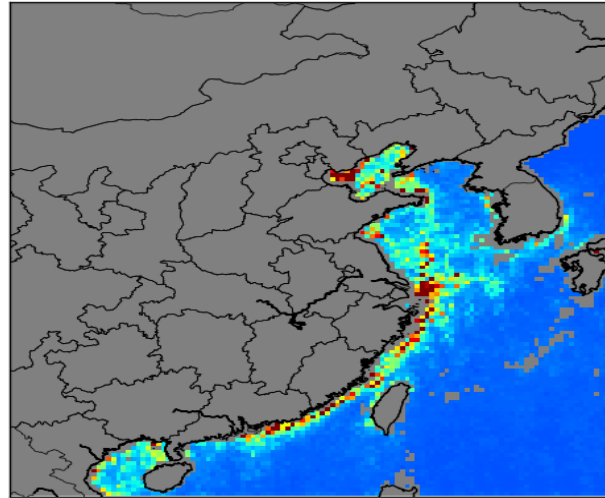
Maritime Emissions – NO_x/CO₂

NO₂ concentrations - OMI



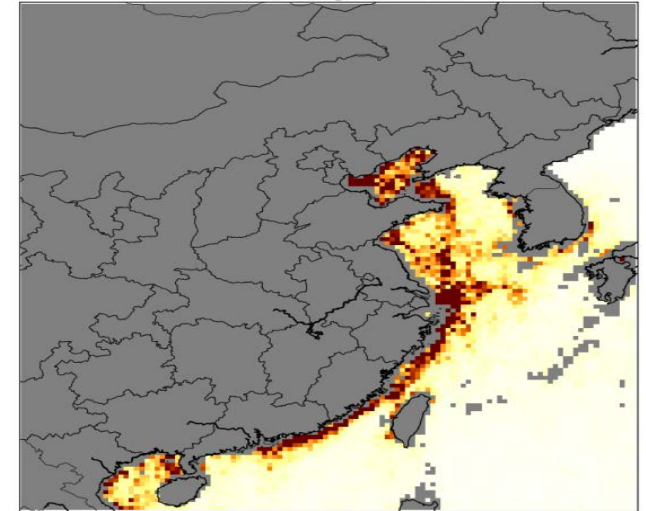
0 1 2 3 4 5 6 7 8 9 10
(a) 10^{15} molecule cm^{-2}

NO_x emissions



0.0 0.1 0.2 0.3 0.4 0.5 0.6 0.7 0.8 0.9 1.0
(b) Gg N grid⁻¹ yr⁻¹

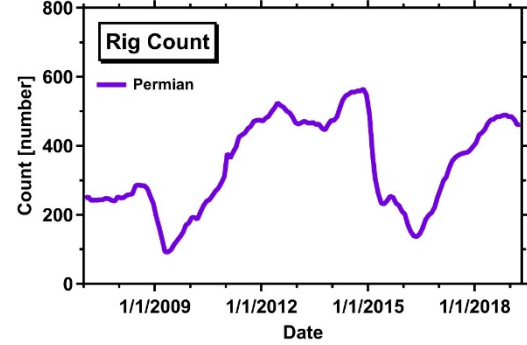
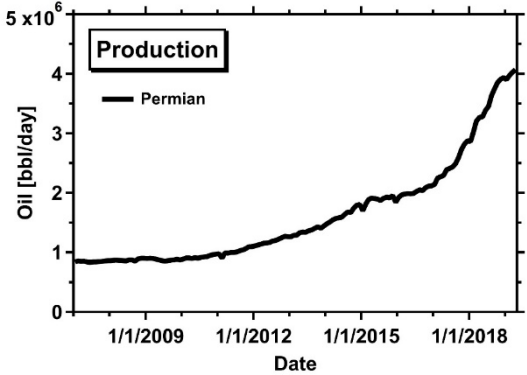
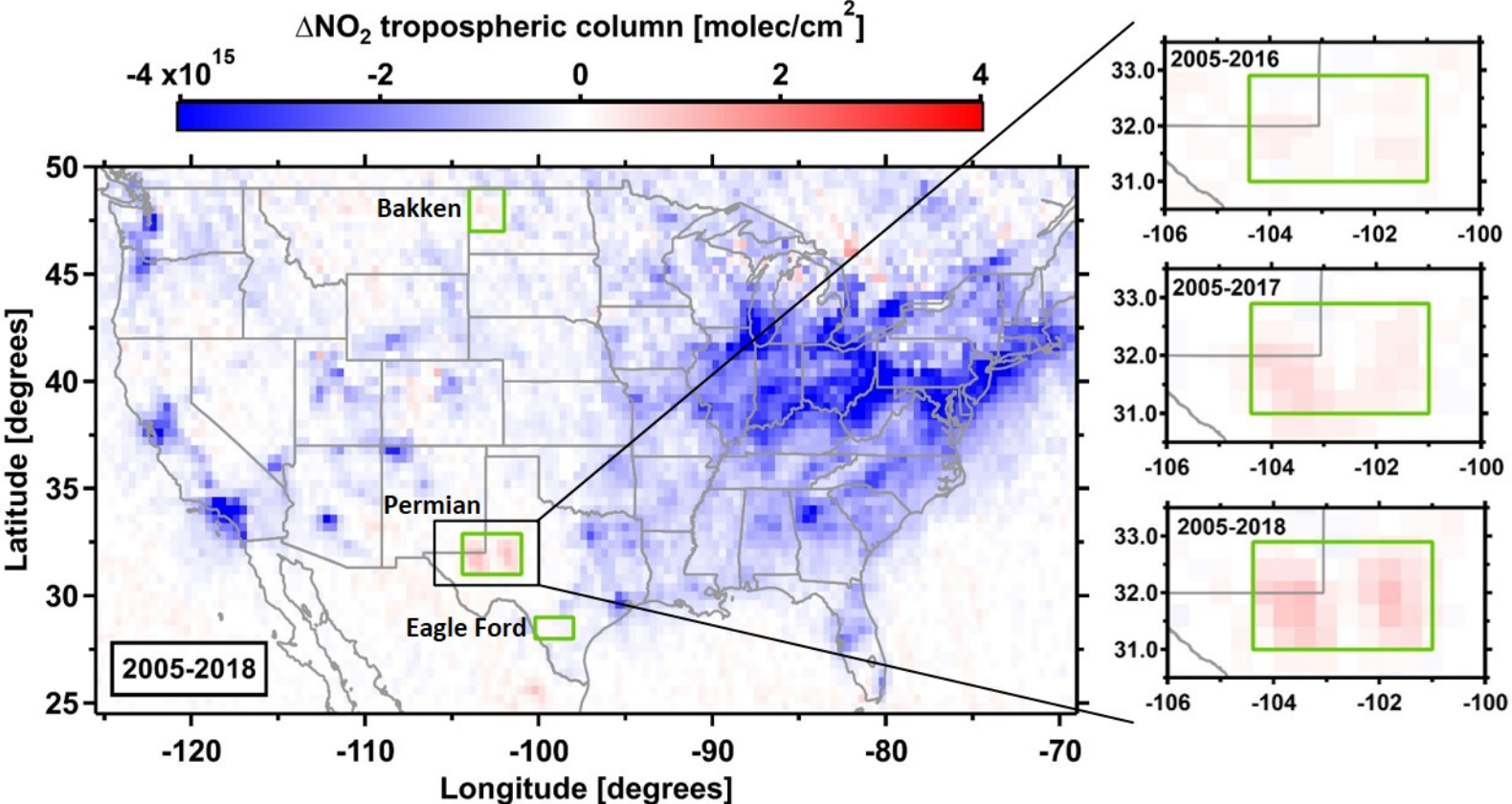
CO₂ emissions



0 10 20 30 40 50 60 70 80 90 100
Mg CO₂ km⁻² Year⁻¹

- Satellite-derived maritime NO_x emissions are revealed that were hidden below the NO₂ outflow of the Chinese mainland.
- The NO_x emissions are derived from OMI observations with the KNMI algorithm DECSO.
- The known NO_x/CO₂ ratio of ship emissions are used to derive CO₂ emissions of ships.

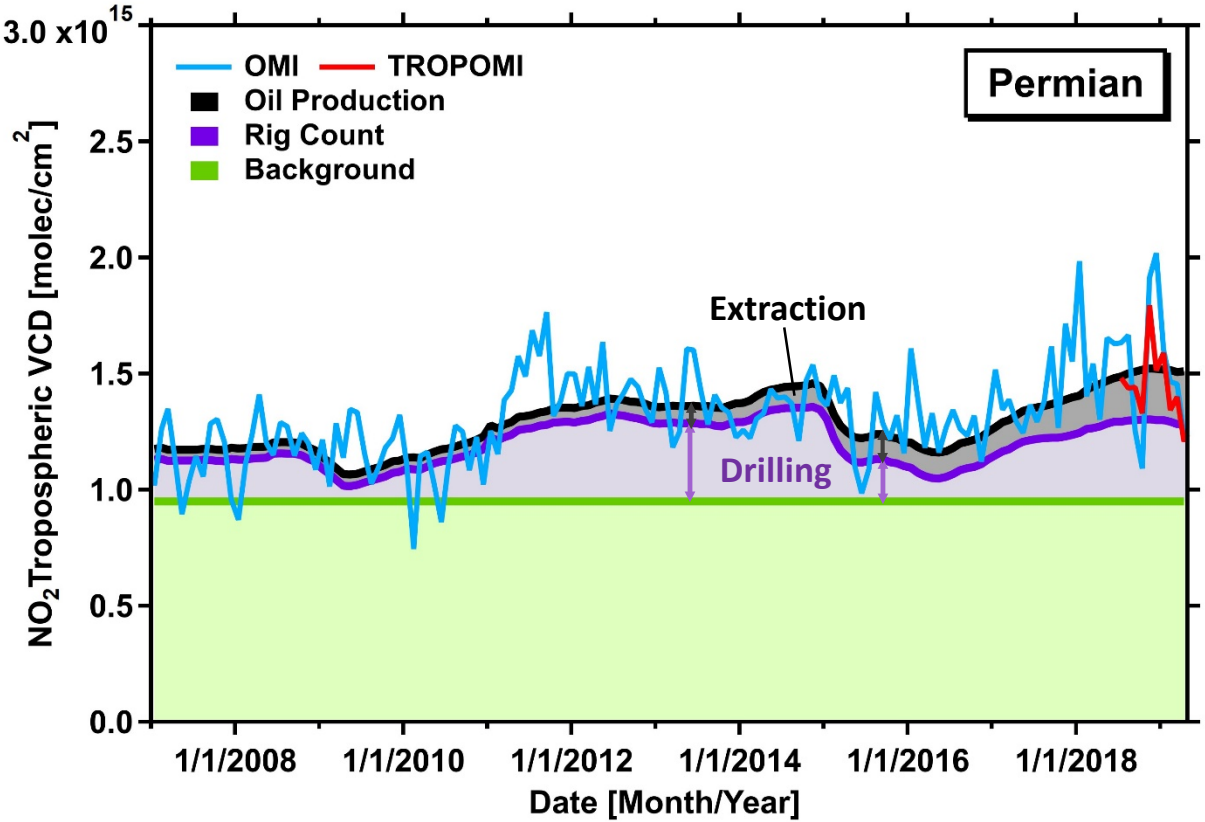
Nitrogen Oxide emissions from U.S. Oil and Gas Production: Recent Trends



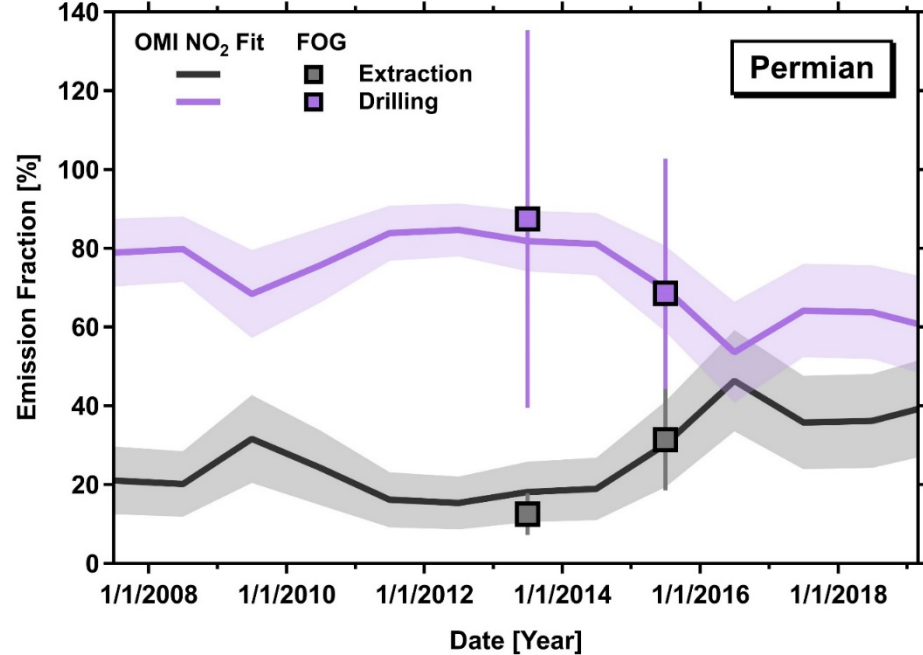
U.S. Energy Information Agency

OMI NO_2 tropospheric VCD product (QA4ECV version 1.1, KNMI)

Nitrogen Oxide emissions from U.S. Oil and Gas Production: Source Attribution



Top down and bottom up source attribution



Multivariate regression on OMI NO₂ time series:

$$NO_2 = a \times \text{Background} + b \times \text{Rig Count} + c \times \text{Production}$$

Fuel-Based Oil & Gas (FOG) NO_x inventory



OMI's "Fitbit"

- The instrument status is very good
- The calibration status is very good
- The instrument degradation is very slow
- No issues (except for the row anomaly)
- Science data is of very high quality



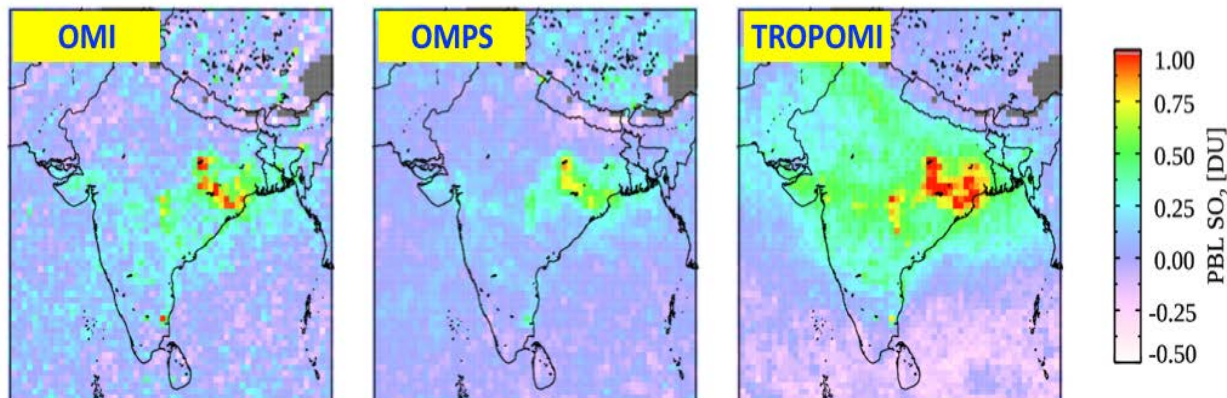
Outlook

- The Instrument Operations Team and the Calibration Team expects to operate the instrument without any problems for the next coming years

OMI: Looking Forward

OMI aging gracefully, contributing to science goals

- Scientists continue to publish with OMI data at high rate.
- Uses by applications community continue to grow.
- Data records are +15 years, trend-quality, some unique.
- OMI-type records continue with OMPS (NASA/NOAA) and TROPOMI (ESA).
- Creating multi-sensor long-term records is not trivial (e.g., OMI-TROPOMI) - many users prefer to stick with OMI for trend analyses
- Air quality measurements are increasingly used in the climate domain and might lead to backward calculations on eg CO₂ emissions



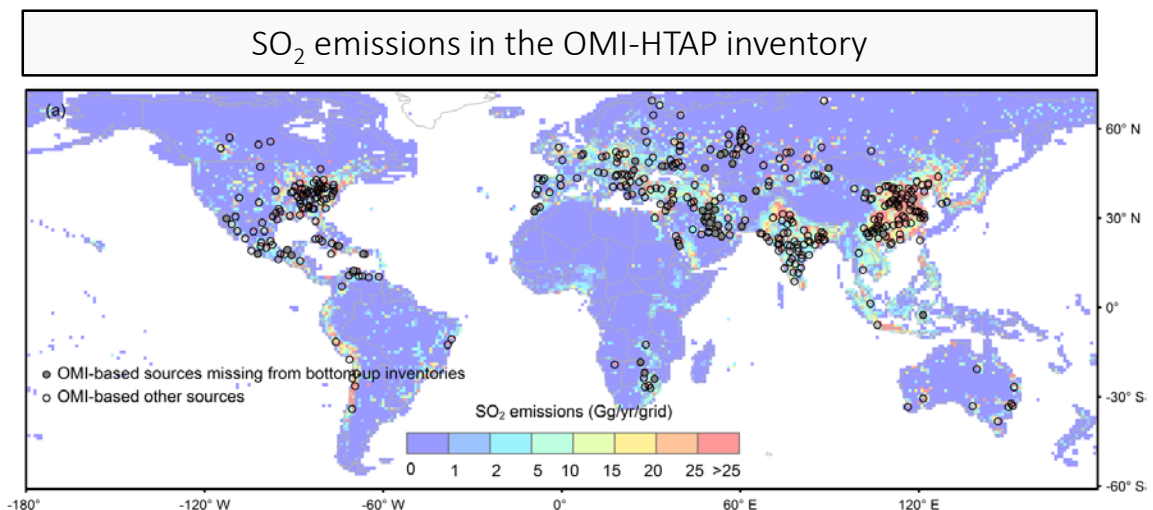
Monthly mean planetary boundary layer SO₂ in April 2018. Differences are related to both instrumental (spatial resolution) and algorithmic factors and are being investigated.



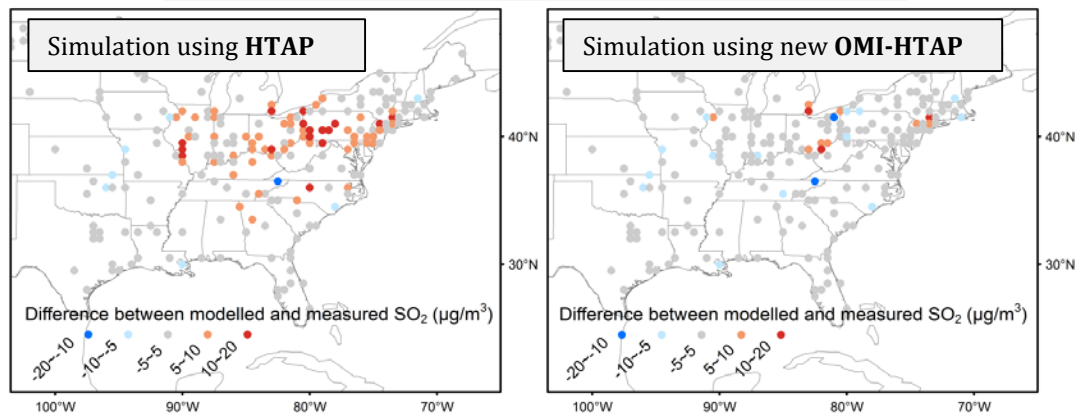
backup

OMI science: Monitoring global air pollution

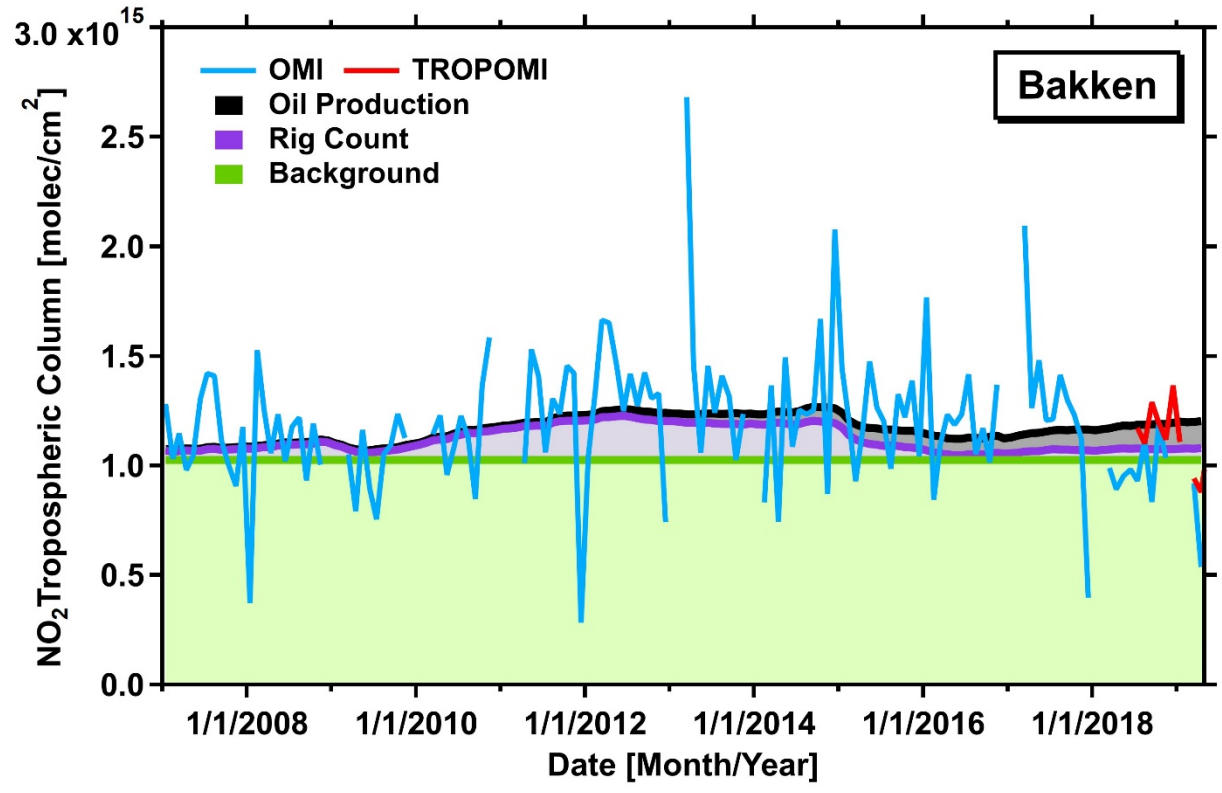
- Emissions from over 400 sources **(including some missing from leading inventories)** from OMI, accounting for ~50% of reported anthropogenic SO₂ emissions.
- **A new emission inventory, OMI-HTAP**, combines OMI-based SO₂ emissions for large sources and the bottom-up inventory, HTAP, for smaller sources.
- OMI-HTAP: (1) **timely** emissions from OMI-detected sources and (2) improves chemistry & transport modeling, e.g., over the US (on right) where emissions have been dropping.
Lu, F., et al., Atmos. Chem. Phys., 18, 2018.



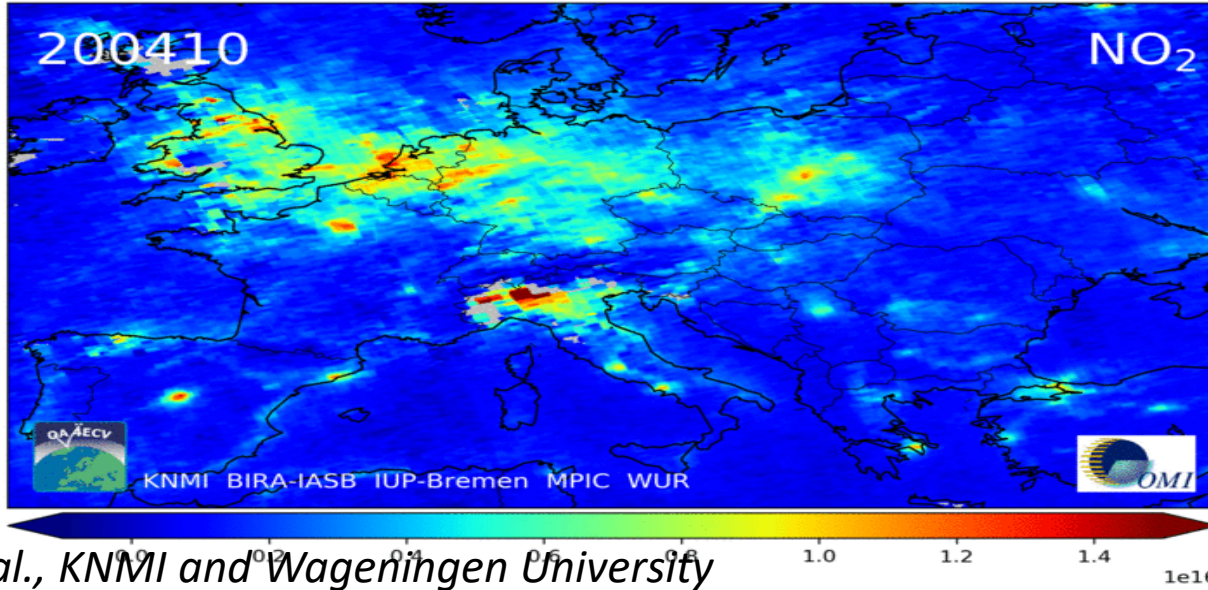
Improved model performance with the new emission product OMI-HTAP



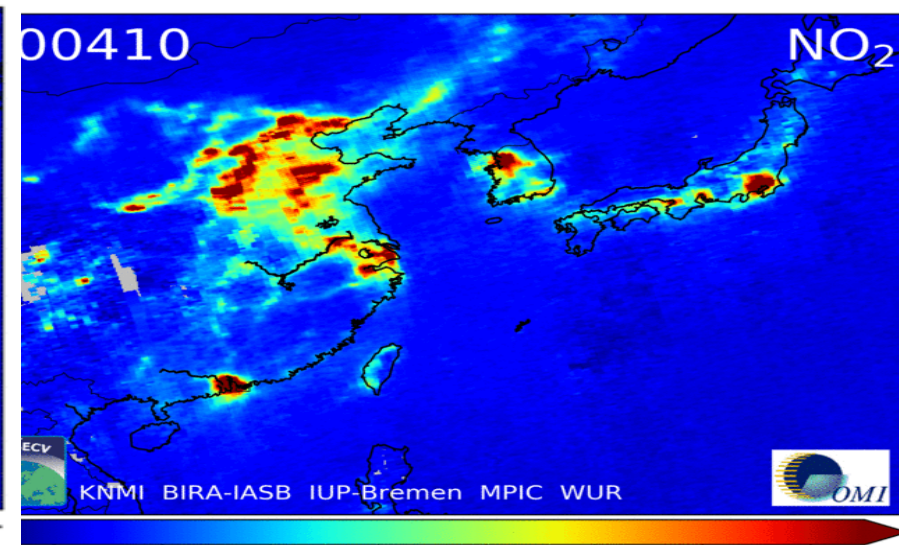
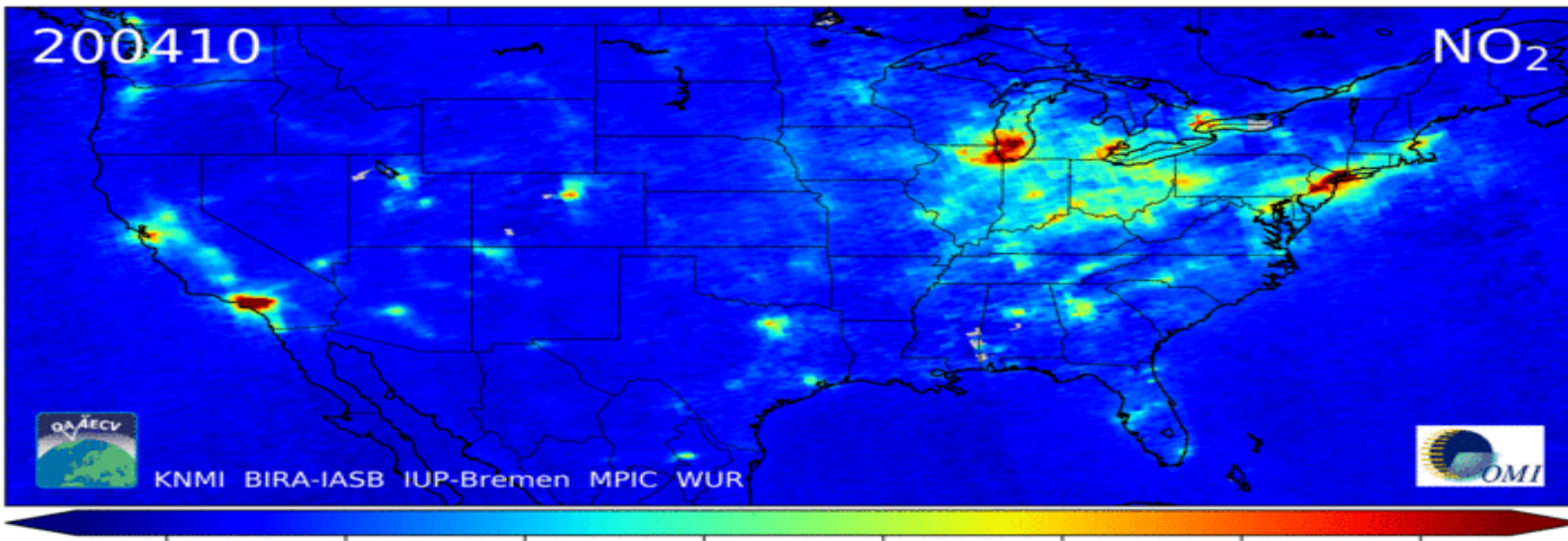
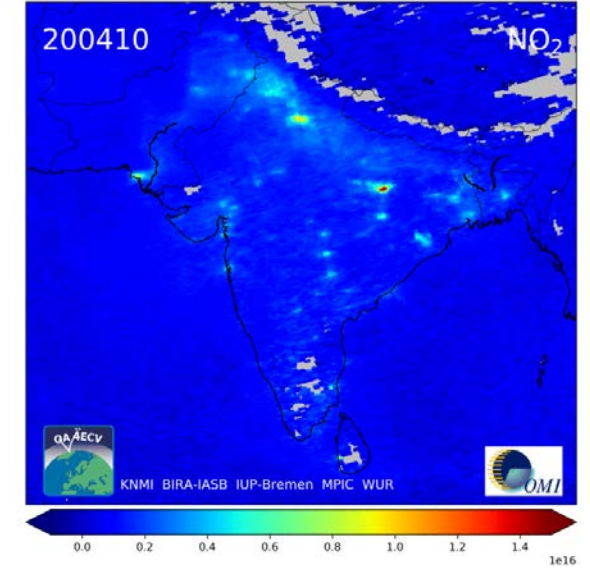
Differences of 2010 annual averaged surface SO₂ between in-situ & NASA-modeled SO₂



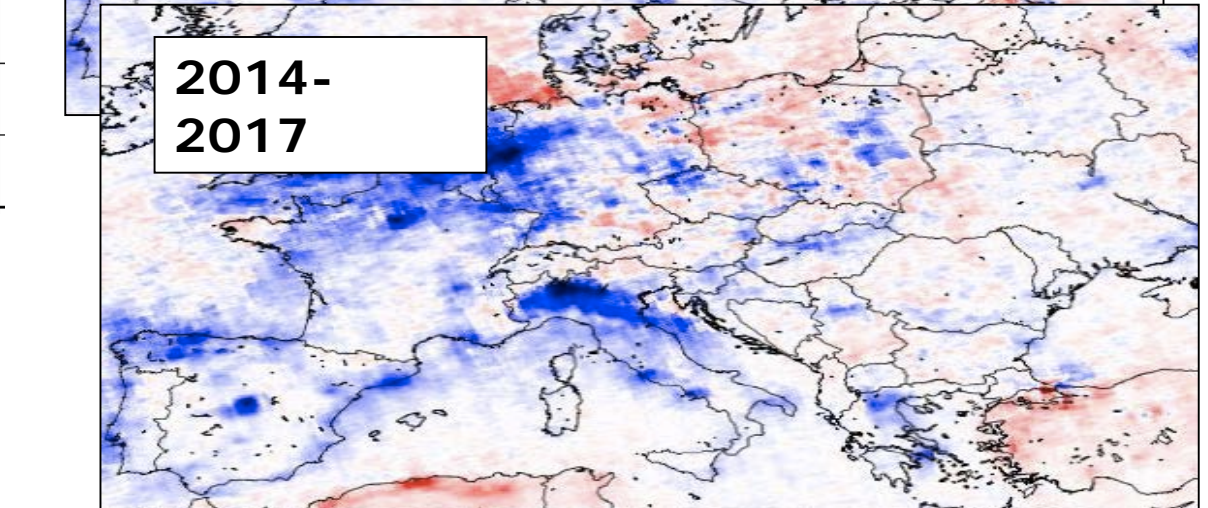
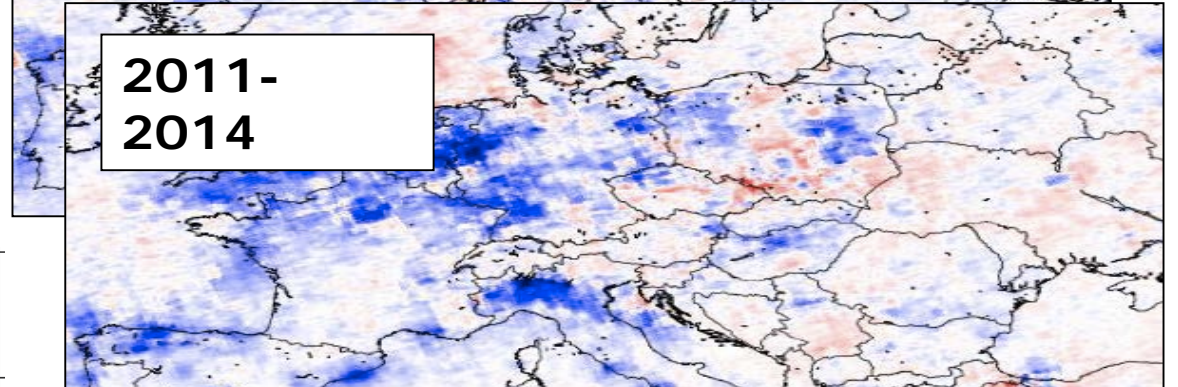
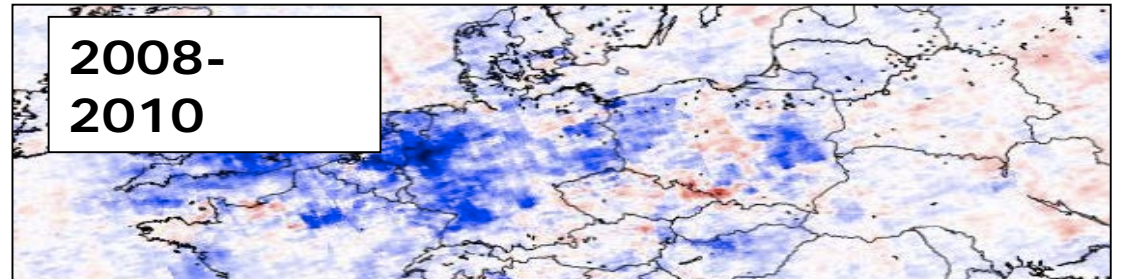
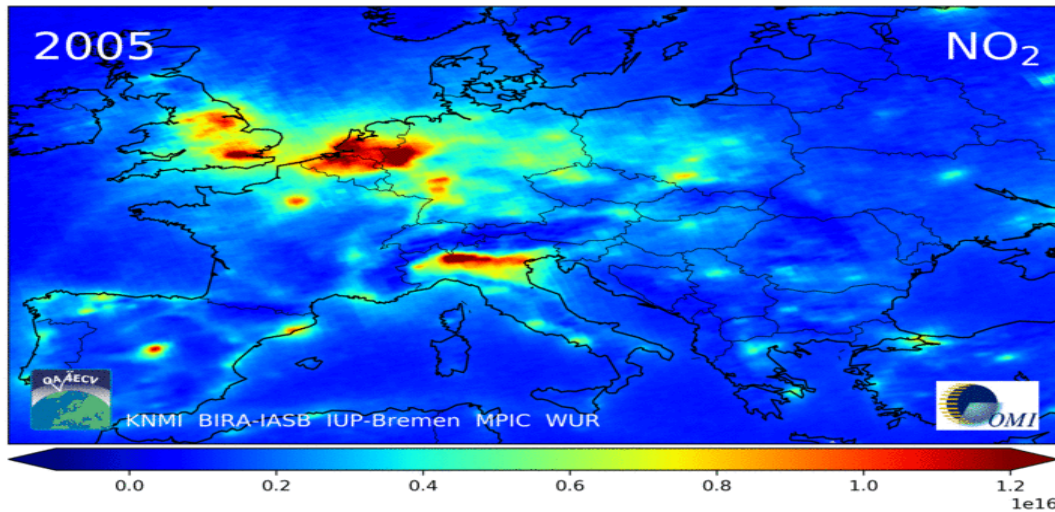
What about the future of OMI?



Zara et al., KNMI and Wageningen University



OMI Nitrogen Dioxide trend in Europe



	2005-2007	2008-2010	2011-2013	2014-2017
London	13.3±0.2	10.7±0.2	10.5±0.2	8.9±0.1
Amsterdam	11.7±0.1	9.4±0.1	8.8±0.1	8.5±0.08
Paris	10.4±0.3	8.3±0.3	8.3±0.3	6.7±0.2

- New QA4ECV NO₂ data
- Indications for slowdown
- Investigate role of policy and economy

Instrument status
Level 2 product status

Use of OMI for next senior review – TROPOMI:

- Ozone layer and recent increase in CFC 11
- Operational use of OMI in CAMS
- Trends
- Health community
- VFD
- Solar Irradiance for solar community

Info van Folkert

Use of OMI for next senior review – TROPOMI:

- Ozone layer and recent increase in CFC 11
- Operational use of OMI in CAMS
- Trends
- Health community
- VFD
- Solar Irradiance for solar community

Antarctic ozone hole

Ozone Mass Deficit every year on 14 September

KNMI Multi Sensor Reanalysis (MSR)

(incl. OMI total ozone, dominant/best satellite source in MSR since 2004)

